9. Particle Identification

9.1 Introduction

9.2 Particle Identification via Time of Flight

9.3 Particle Identification via Ionization measurement (dE/dx)

9.4 Cherenkov Detectors

9.5 Transition Radiation Detectors

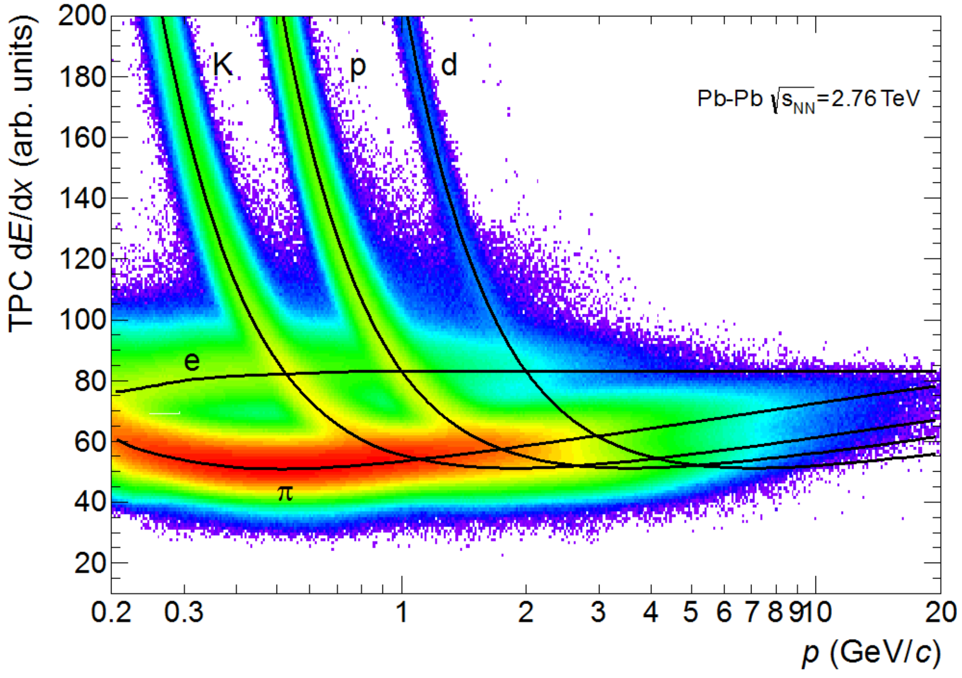

9.1 Introduction

- In addition to tracking and calorimetry, detectors for particle identification are crucial elements in many particle physics experiments

- Stable particles are identified by:

  (i) Their type of interaction with matter
  (e, γ, μ, hadrons)

  (ii) By measuring their mass
  (mass → particle)

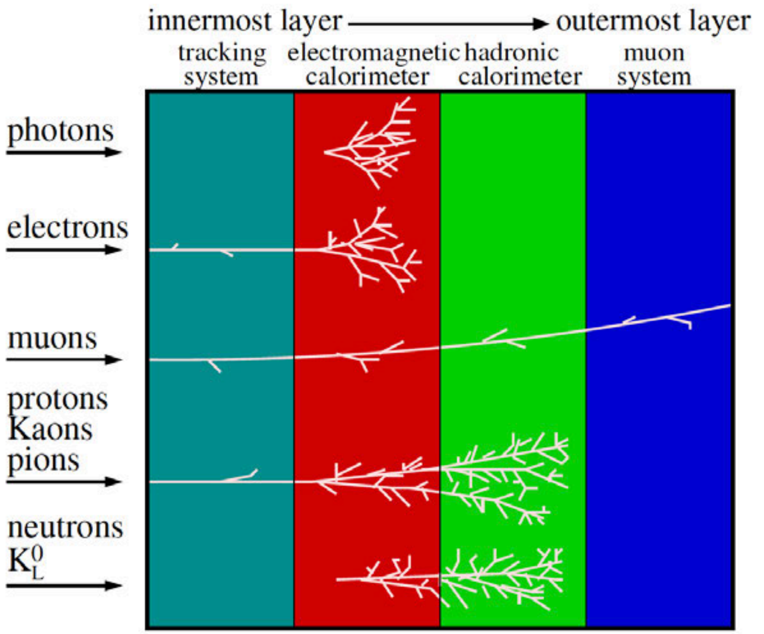

- The second method is most relevant to separate hadrons (π, K, p, …)

  (their type of interaction is the same, no discrimination power)

- The measurement of the mass requires the measurement of either the velocity β (or Lorentz factor γ) in addition to the momentum measurement

$$\boxed{p = \gamma m \beta c}$$

- The measurement of velocity requires a second measurement, a second independent detector signature

- Various possibilities exist to identify/ separate charged hadrons (see also Section 2):

  (i) Direct measurement of β (or γ):

Time of flight:	$\Delta t \sim 1/\beta$
Cherenkov angle:	$\cos\theta_C = 1 / \beta n$
Transition radiation:	$\sim \gamma$ ($\gamma > 100$)

  (ii) Energy loss (Bethe-Bloch)

  $$\boxed{\frac{dE}{dx} \propto \frac{z^2}{\beta^2} \ln(a\beta\gamma)}$$

- Neutral hadrons are more difficult to separate; stable are: n (→ calorimeter)

  Long-lived neutral strange hadrons: V_0 decays → reconstruct from decay kinematics (invariant mass)

→ The challenge is $\pi^{\pm}$, $K^{\pm}$, p separation

- The mass m can be reconstructed from the momentum and β measurement:

$$m = \frac{p}{c\beta\gamma}$$

- The uncertainty is given by:

$$\left(\frac{\mathrm{d}m}{m}\right)^2 = \left(\frac{\mathrm{d}p}{p}\right)^2 + \left(\gamma^2 \frac{\mathrm{d}\beta}{\beta}\right)^2$$

- Since in most cases $\gamma >> 1$, the mass resolution is determined by the accuracy of the velocity measurement

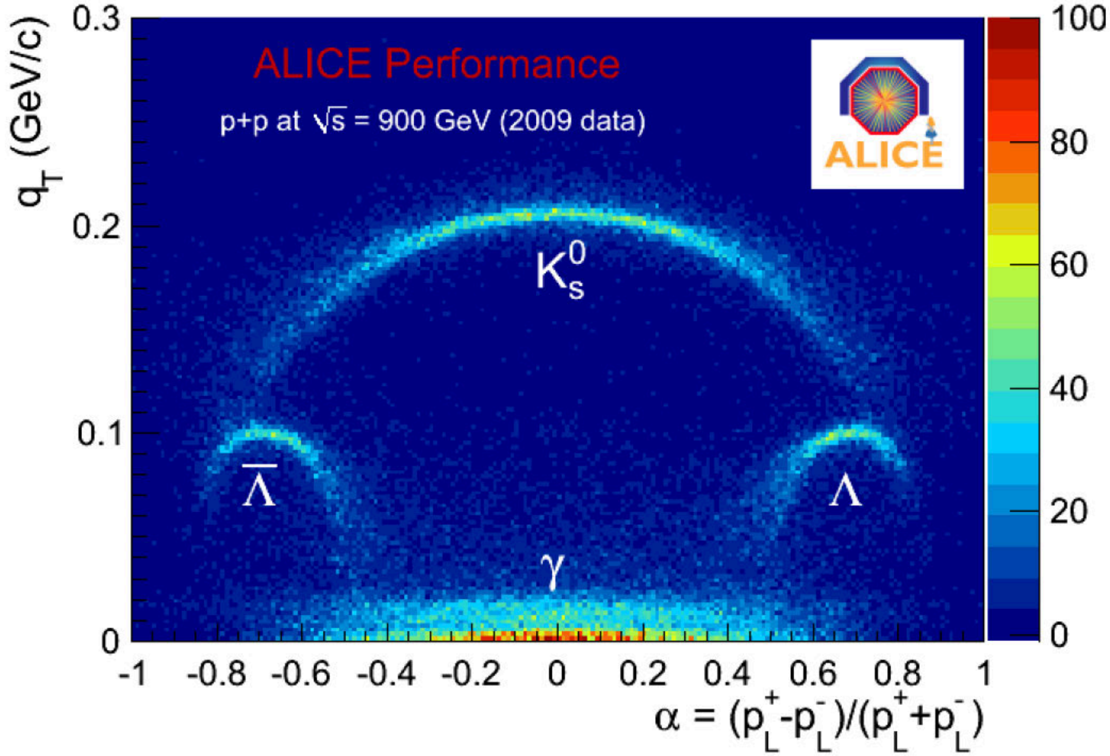

Armenteros plot from the ALICE experiment using data from $\sqrt{s}$ = 900 GeV pp collisions. The different V_0 particles can be separated using the kinematic properties of their decay products.

$p_L^{\pm}$: Longitudinal momenta of the positively and negatively charged decay product in the direction of flight of the V_0 (momentum vector)

q_T : Transverse component of the momentum of the positive decay product

Demonstration of the power of Particle Identification

Example 1: $\phi \rightarrow K^+ K^-$ decays

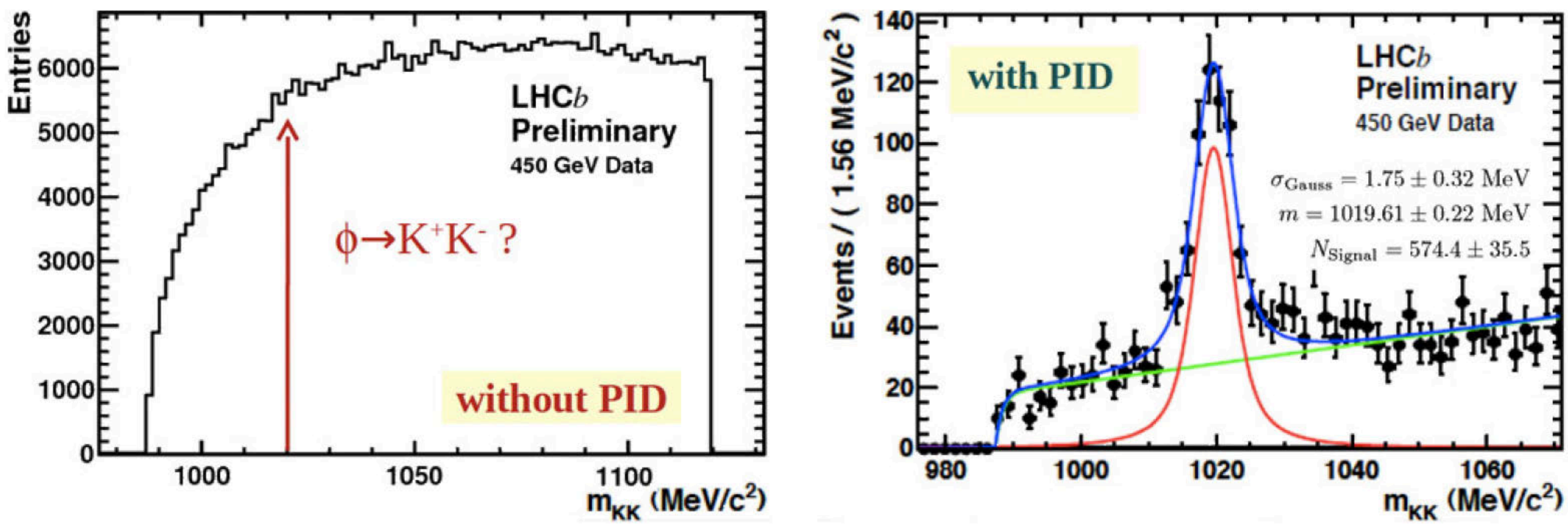

Search for $\phi \rightarrow K^+ K^-$ decays in the LHCb experiment
Left: Invariant mass of all pairs of tracks, without particle ID
Right: Invariant mass of all pairs of identified charged kaons using a Cherenkov detector

The inclusive decay $\phi \rightarrow K^+ K^-$ only becomes visible after particle (kaon) identification

Example 2: Measurement of rare B decays, e.g.: $B_d^0 \rightarrow \pi^+ \pi^-$

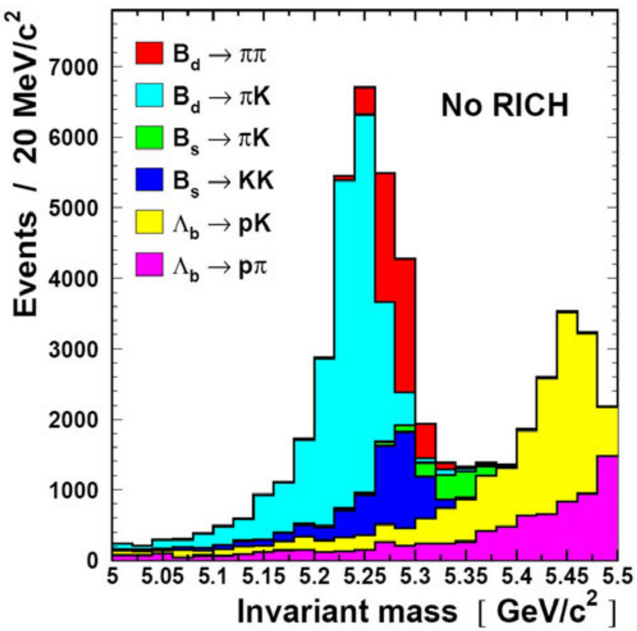

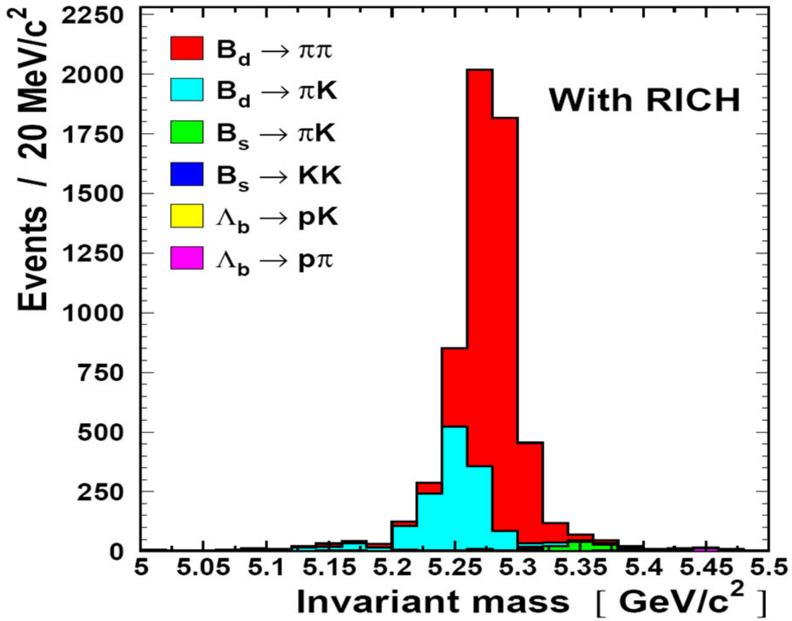

Reconstructed two-particle masses (Monte Carlo simulation, LHCb experiment)
Left: Without particle ID, assuming pion hypotheses
Right: With particle ID, using p / K / p separation in a Ring Image Cherenkov Counter (RICH)

Rare decays become accessible after particle identification (π, K, p separation)

9.2 Time-of-flight measurement

- Basic idea: measure the time difference between the interaction and the passage of a particle through a Time-of-flight (TOF) counter (or the time difference between two detectors with a good time resolution)

- Traditionally: Plastic Scintillator + PMTs

  Typical resolution: ~100 ps π/K separation up to ~1.5 GeV.

- To go beyond that: one needs faster detectors:

  → Use Cherenkov light (prompt) instead of scintillations

  → Use fast gas detectors e.g. Resistive Plate Chambers (RPC)

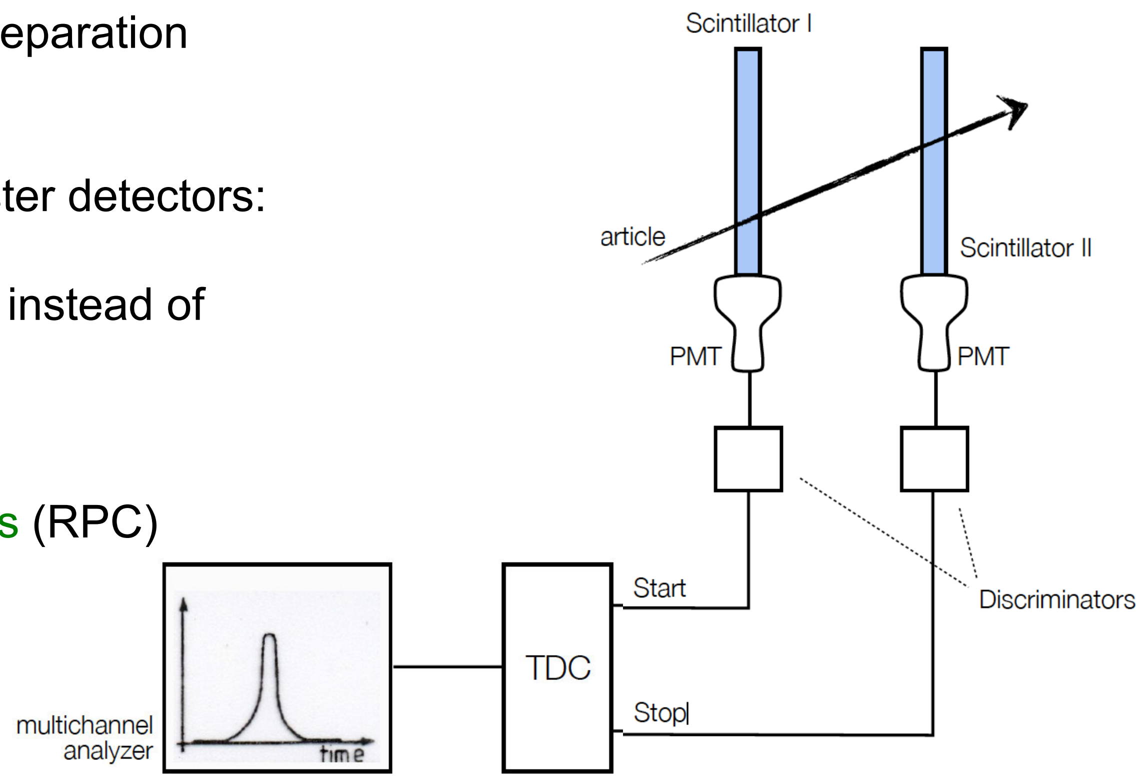

Calculation of time differences / required time resolutions

Distinguishing particles with ToF:
[particles have same momentum p]

Particle 1 : velocity v_1, β_1; mass m_1, energy E_1
Particle 2 : velocity v_2, β_2; mass m_2, energy E_2

Distance L : distance between ToF counters

$$\Delta t = L\left(\frac{1}{v_1} - \frac{1}{v_2}\right) = \frac{L}{c}\left(\frac{1}{\beta_1} - \frac{1}{\beta_2}\right)$$

$$= \frac{L}{pc^2}(E_1 - E_2) = \frac{L}{pc^2}\left(\sqrt{p^2c^2 + m_1^2c^4} - \sqrt{p^2c^2 + m_2^2c^4}\right)$$

Relativistic particles, $E \simeq pc \gg m_i c^2$:

$$\Delta t \approx \frac{L}{pc^2}\left[\left(pc + \frac{m_1^2c^4}{2pc}\right) - \left(pc + \frac{m_2^2c^4}{2pc}\right)\right]$$

$$\Delta t = \frac{Lc}{2p^2}\left(m_1^2 - m_2^2\right)$$

For L = 2 m:

Requiring $\Delta t \gtrsim 4\sigma_t$ K/π separation possible up to p = 1 GeV if $\sigma_t \approx 200$ ps ...

Cherenkov counter, RPC : $\sigma_t \approx 40$ ps ...
Scintillator counter : $\sigma_t \approx 80$ ps ...

Example:

Pion/Kaon separation ...
[$m_K \approx 500$ MeV, $m_\pi \approx 140$ MeV]

Assume:
p = 1 GeV, L = 2 m ...

$$\rightarrow \quad \Delta t \approx \frac{2\ \mathrm{m} \cdot c}{2\ (1000)^2\ \mathrm{MeV}^2/c^2}\left(500^2 - 140^2\right)\ \mathrm{MeV}^2/c^4$$

$$\approx 800\ \mathrm{ps}$$

Separation power (in standard deviations) of Time-of-Flight measurements

For two particles with masses m_1 and m_2 with the same momentum p, the separation power in numbers of GaussianStandard deviations is given by:

$$n_{\sigma_{TOF}} = \frac{|t_1 - t_2|}{\sigma_{TOF}} = \frac{Lc}{2p^2\sigma_{TOF}} |m_1^2 - m_2^2|$$

→ separation power above 3σ in the low momentum range,
e.g. π/K separation with > 3σ for p < 1.6 GeV (2.3 GeV) for a time resolution of 100 ps (50 ps)

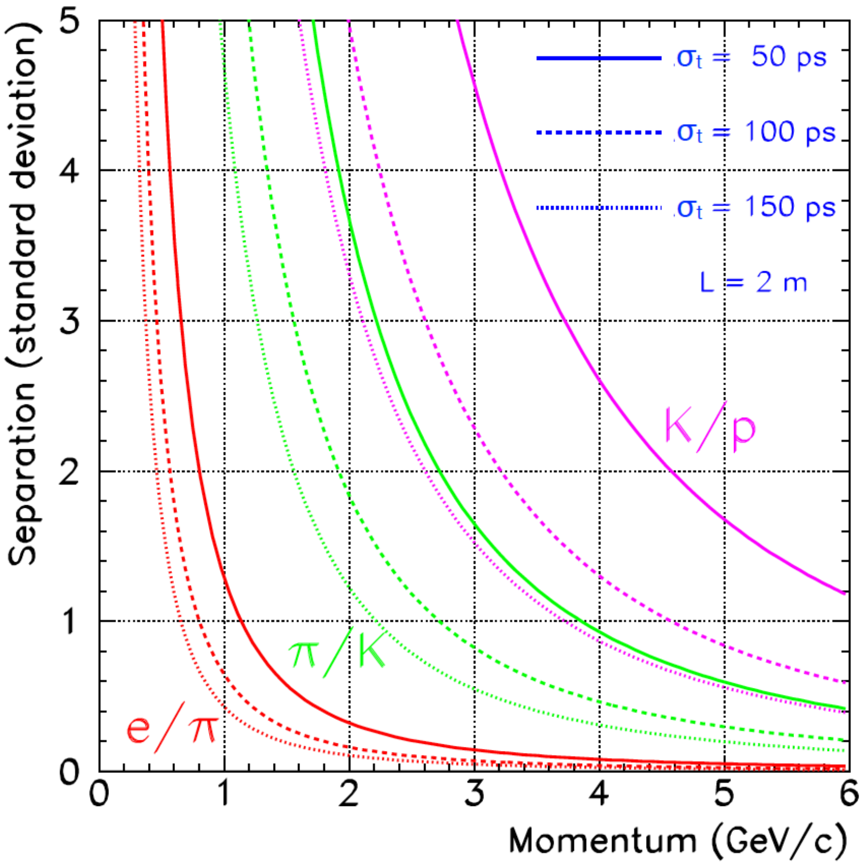

Particle separation with TOF measurements for three different system time resolutions (σ_{TOF} = 50, 100, 150 ps) and for a flight length of L = 2m)
[no uncertainties on p and L assumed]

Calculation of mass resolution

Use: $\beta = L/\tau$
$\gamma = (1-\beta^2)^{-1}$
$[c=1]$

$$p = \beta\gamma m$$

$$m^2 = p^2\left(\frac{1}{\beta^2}-1\right) = p^2\left(\frac{\tau^2}{L^2}-1\right)$$

$$\text{*}\quad \frac{p^2\tau^2}{L^2} = m^2 + p^2 = E^2$$

$$\rightarrow\quad \delta(m^2) = 2p\,\delta p\underbrace{\left(\frac{\tau^2}{L^2}-1\right)}_{m^2/p^2} + \underbrace{2\tau\delta\tau\frac{p^2}{L^2} - 2\frac{\delta L}{L^3}p^2\tau^2}_{\text{use *}}$$

$$= 2m^2\frac{\delta p}{p} + 2E^2\frac{\delta\tau}{\tau} - 2E^2\frac{\delta L}{L}$$

$$\rightarrow\quad \sigma(m^2) = 2\left[m^4\left(\frac{\sigma_p}{p}\right)^2 + E^4\left(\frac{\sigma_\tau}{\tau}\right)^2 + E^4\left(\frac{\sigma_L}{L}\right)^2\right]^{1/2}$$

Usually:

$$\left.\frac{\delta L}{L} \ll \frac{\delta p}{p} \ll \frac{\delta\tau}{\tau}\right] \quad\rightarrow\quad \sigma(m^2) = 2E^2\,\frac{\sigma_\tau}{\tau}$$

Uncertainty in time measurement dominates ...

Resistive Plate Chambers (RPC)

- For large systems the coverage with scintillators and photon readout is expensive

- Resistive Plate Chambers provide an efficient and “cheaper” alternative
  (Relatively simple construction, good time resolution)

- Layout:

  - Planar geometry, parallel plates with high resistivity form electrodes (glass, bakelite)

  - Very High voltage, thin gap of typically a few mm, filled with gas → high gas gain

  - Ionisation + very high voltage → avalanche or streamer mode
    (due to high resistivity, large signals or discharges are restricted to a well-localized area)

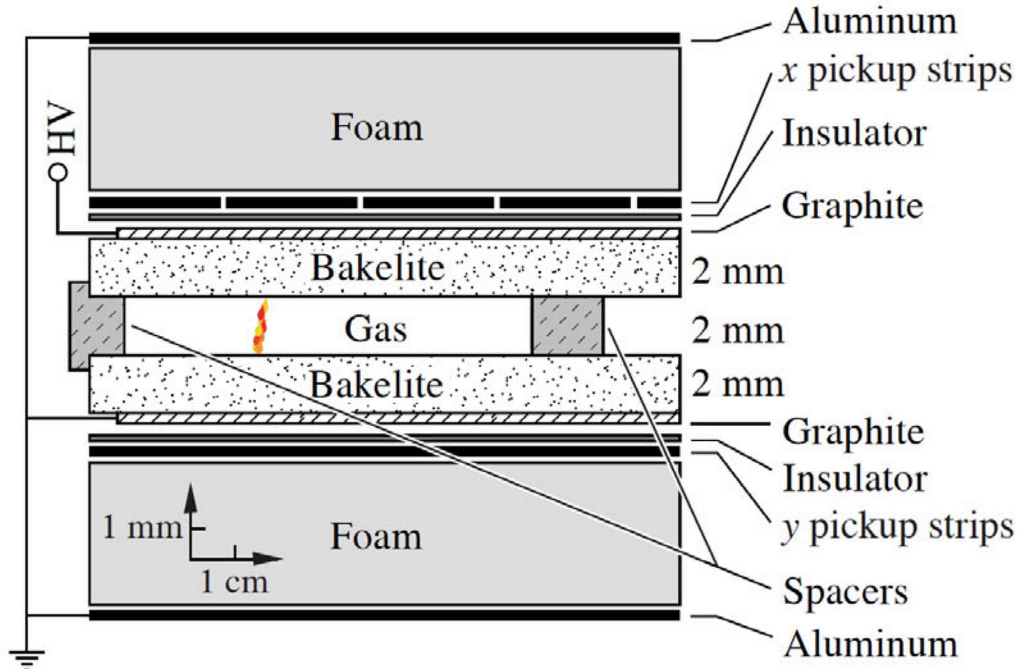

Schematic layout of a resistive plate chamber

- Layout (cont.):

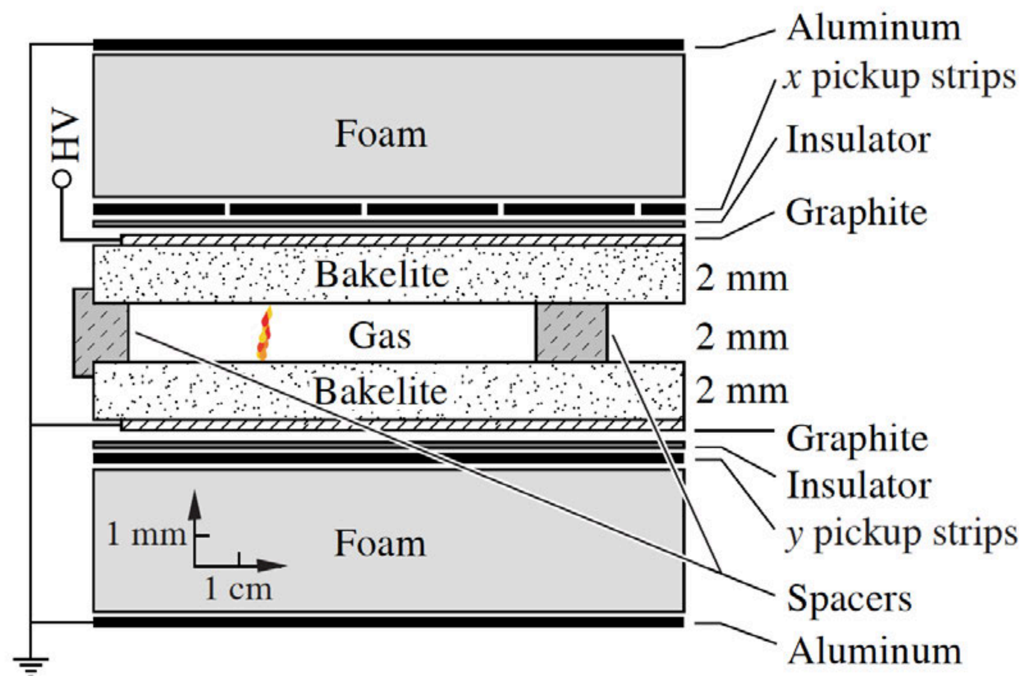

- Planar geometry, parallel plates
  with high resistivity form electrodes
  (glass, bakelite)

- Very High voltage, thin gap of
  typically a few mm, filled with gas.
  → high gas gain

- Ionisation + very high voltage
  → avalanche or streamer mode
  (due to high resistivity, large signals
  or discharges are restricted to a
  well-localized area)

- Strips in orthogonal directions give spatial information (position measurement)

- Accurate time measurement with resolutions of □~50 ns over large areas possible
  up to charged particle rates of a few kHz/cm^2

- Rate limitations due to large charges (distortion of the electric field,
  and local drop of the electric field in the gas gap → hit spot of the detector becomes
  insensitive to further traversing particles; rest of the detector still o.k.)

-

- On the Rate Limitation of RPCs:

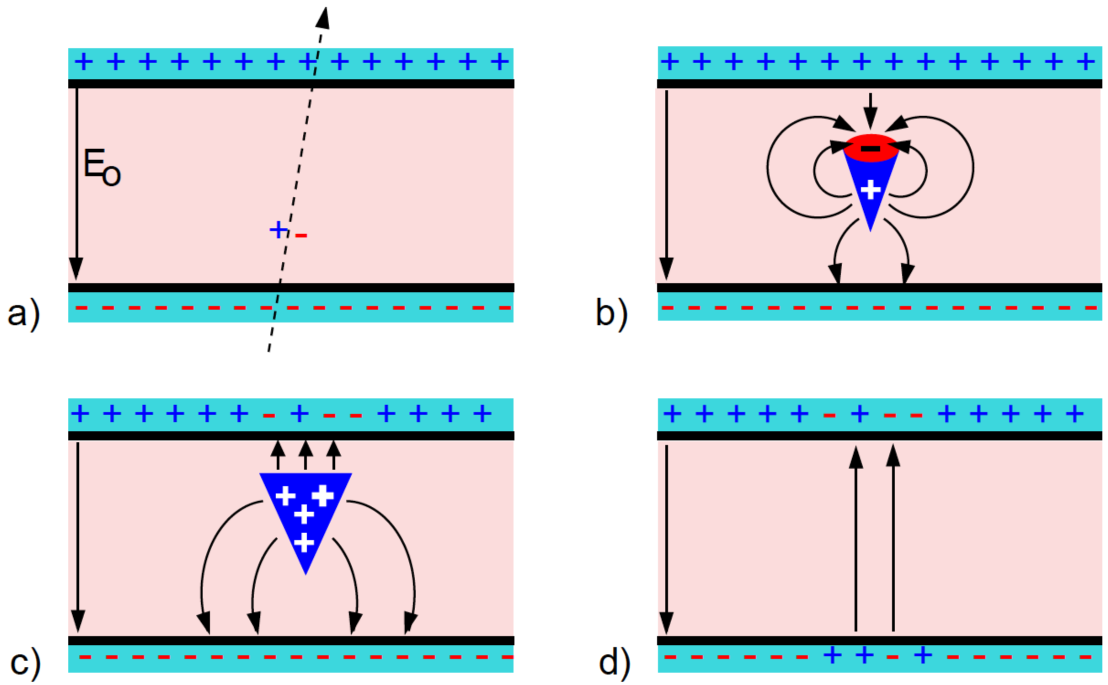

C. Lippmann, PhD thesis, Frankfurt

a) Ionisation of a charged particle
b) Drift inside the electric field, avalanche process
c) Electrons reach anode faster than positive ions
d) Charges on electrodes distort the field, field strength drops below the critical value needed for avalanche creation
   → dead time, due to high resistivity

- RPCs can be operated in Avalanche or Streamer mode

- Avalanche mode: normal Townsend avalanche multiplication

- Large number of charge carriers influences the electric field in the gap and thereby the own amplification

- Higher initial electric fields (~40 kV/cm)
  → higher gas gain
  → larger photon contributions

- Streamer can be formed, conductive channel between the two electrodes

- Streamer mode: large current signals, no amplifying electronics needed

Typical charges: a few nC, high efficiency,
time resolutions of a few ns,
however: larger dead time / rate limitation at a few 100 Hz/cm^2

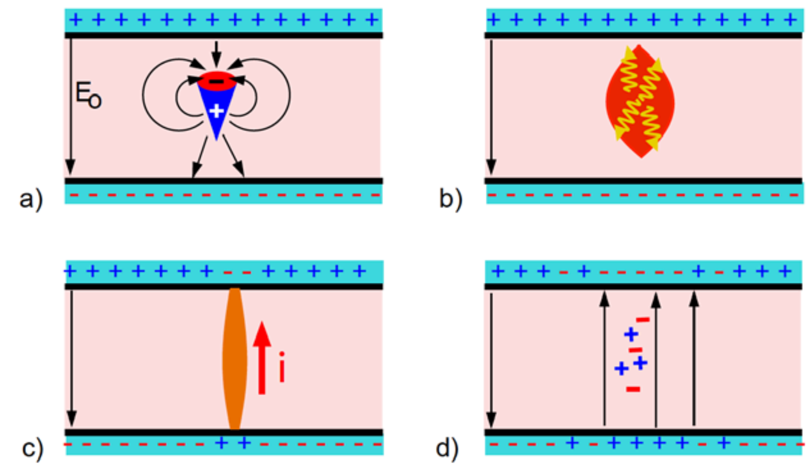

C. Lippmann, PhD thesis, Frankfurt

a) Avalanche in very high fields,
b) Photon contributions from excited gas atoms
c) Streamer / spark formation, local discharge of electrodes
d) Heavily distorted field configuration
   → local insensitivity

- Multi-Gap Resistive Plate Chambers

Main advantages:
Increase of efficiency

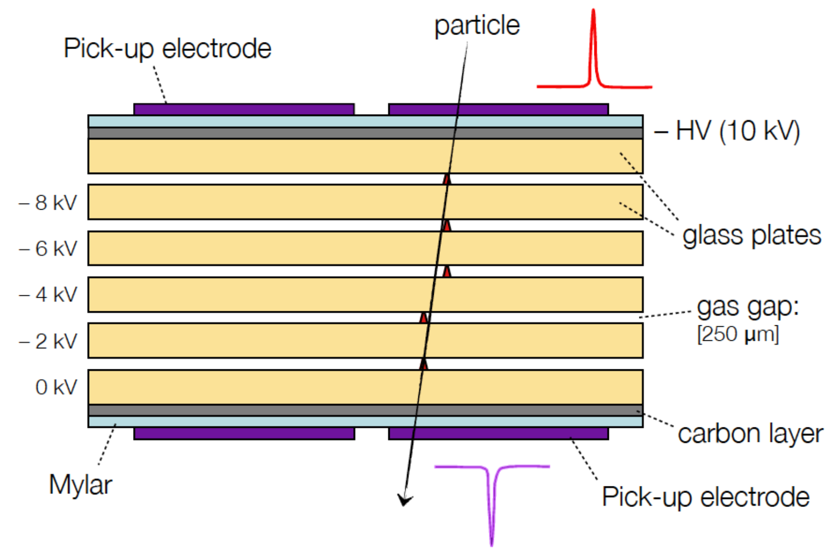

- Stack of equally spaced resistive plates with voltage applied to external surfaces
  → avalanche signals in each gap

- Internal plates are electrically floating

- Electrodes on external surfaces (resistive plates are transparent to induced signals)

Applications of RPCs

Resistive Plate Chambers are heavily used in LHC experiments

(i) ATLAS and CMS:
Fast Muon Trigger Chambers

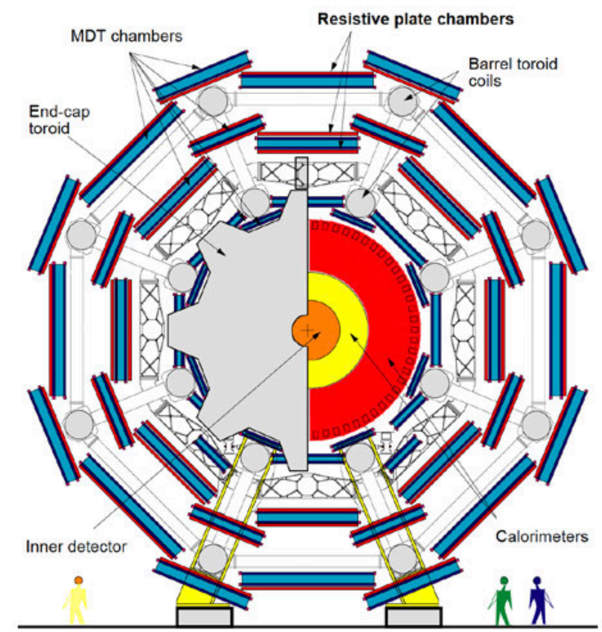

(ii) ALICE:
Time-of-Flight System

Particle ID in high multiplicity environment requires …

ToF system with high granularity and coverage of the full ALICE barrel

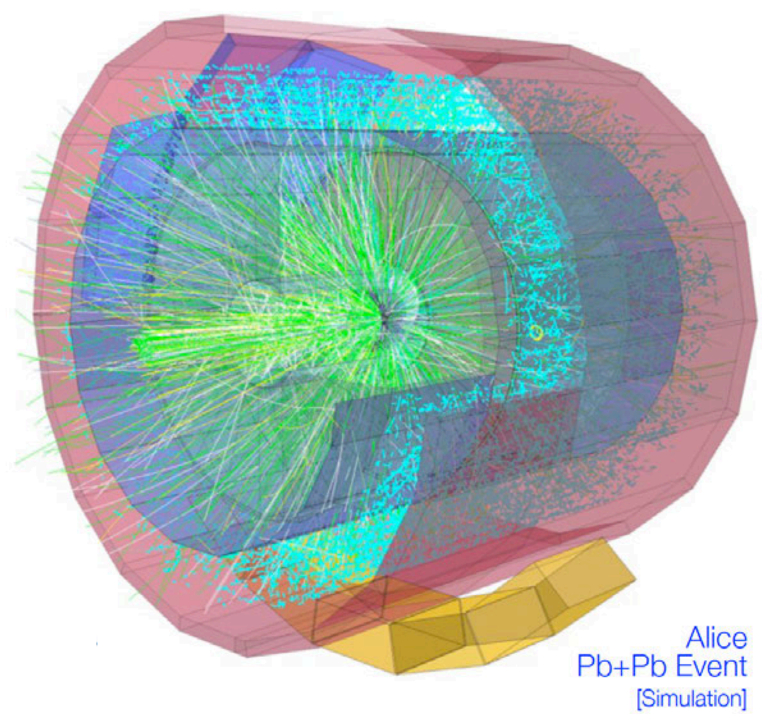

ATLAS RPC Fast Muon Trigger system

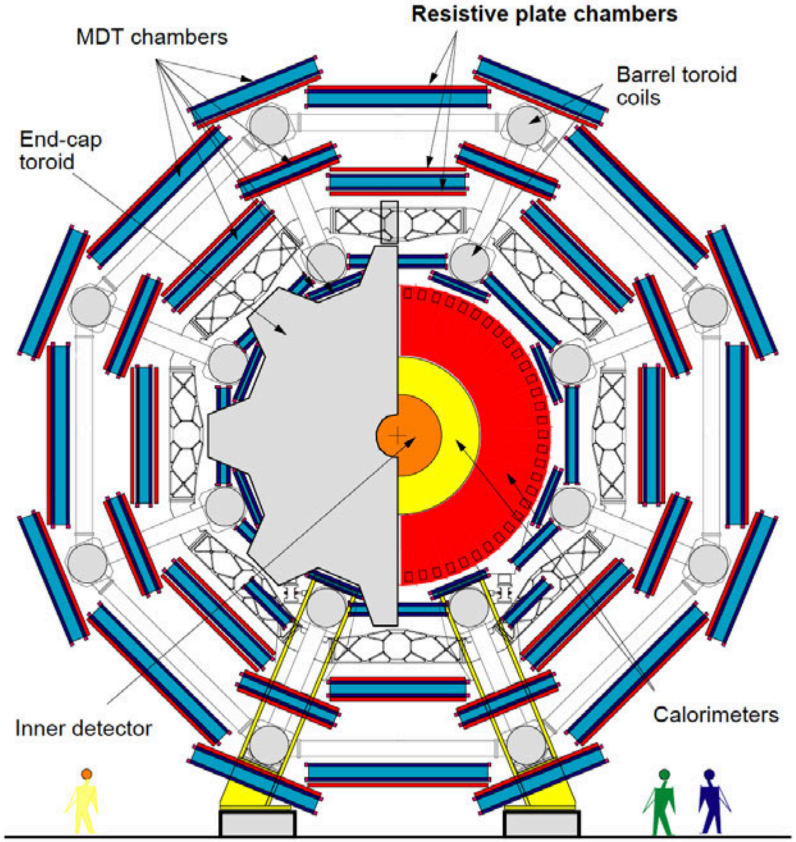

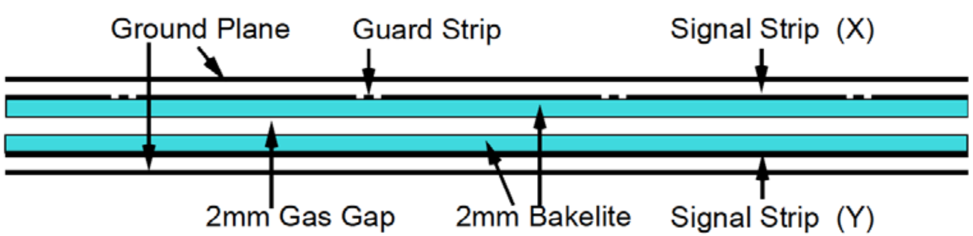

ALICE (Detector for Heavy Ion Collisions at the LHC)

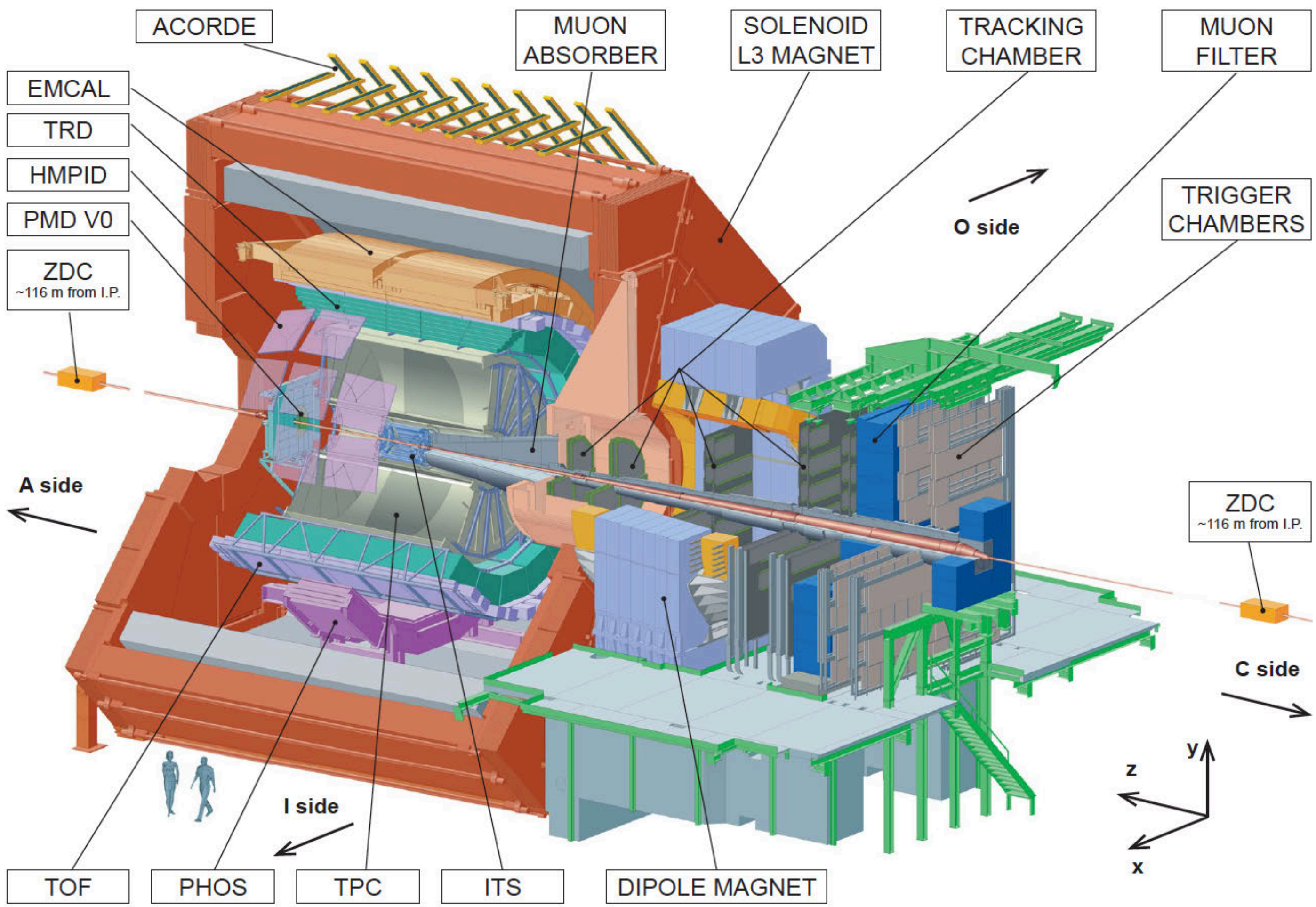

Some focus on Particle Identification (TPC (dE/dx), RPC-based TOF system and a Transition Radiation Detector)

ALICE RPC-based Time-of-Flight system

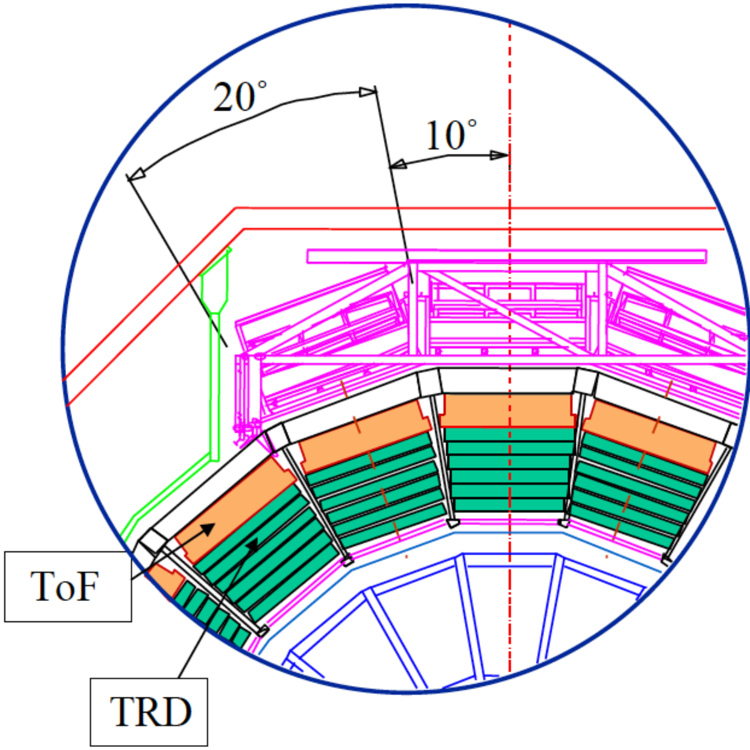

Cross Section
of the ALICE detector

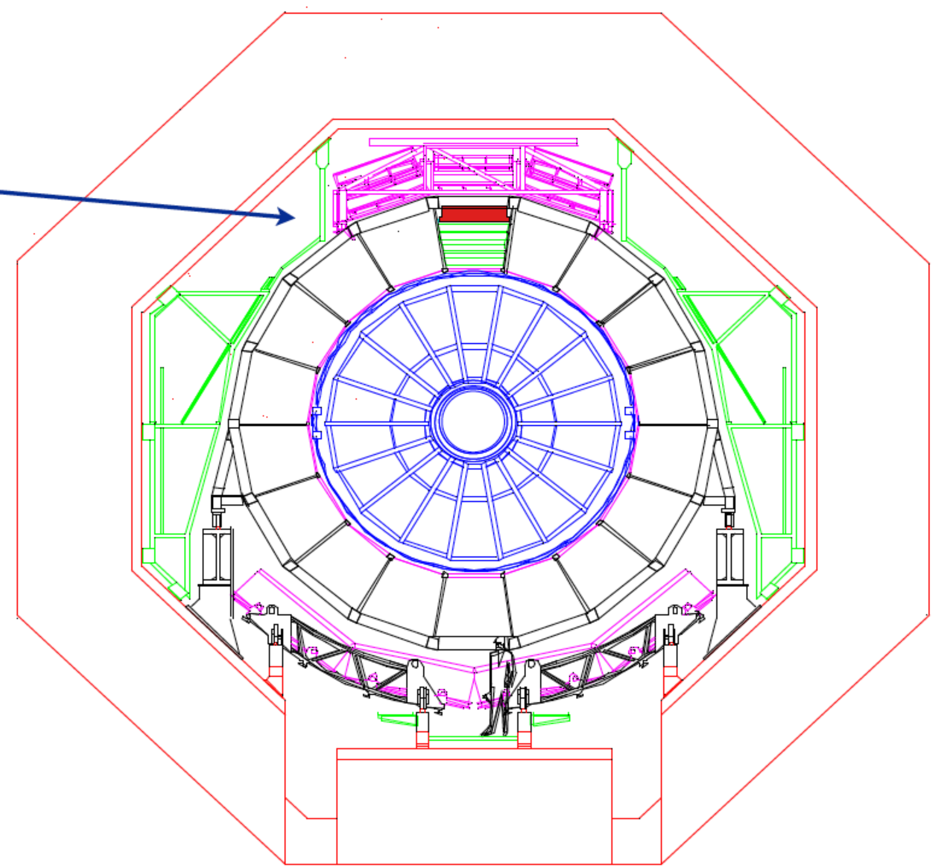

ToF array arranged as
barrel with radius 3.7 m
[Divided into 18 sectors]

→ Large L, good expected separation

ALICE RPC-based Time-of-Flight system

ALICE MRPC
[Time-of-Flight System]

Double stack;
each stack with 5 gaps
[i.e. 10 gaps in total]

250 micron gaps separated
by standard fishing lines

Resistive plates
from soda lime glass
[commercially available]

400 micron internal glass
550 micron external glass

Area: 160 m^2
Channels: 160 k [size: 2.5 x 3.5 cm^2]

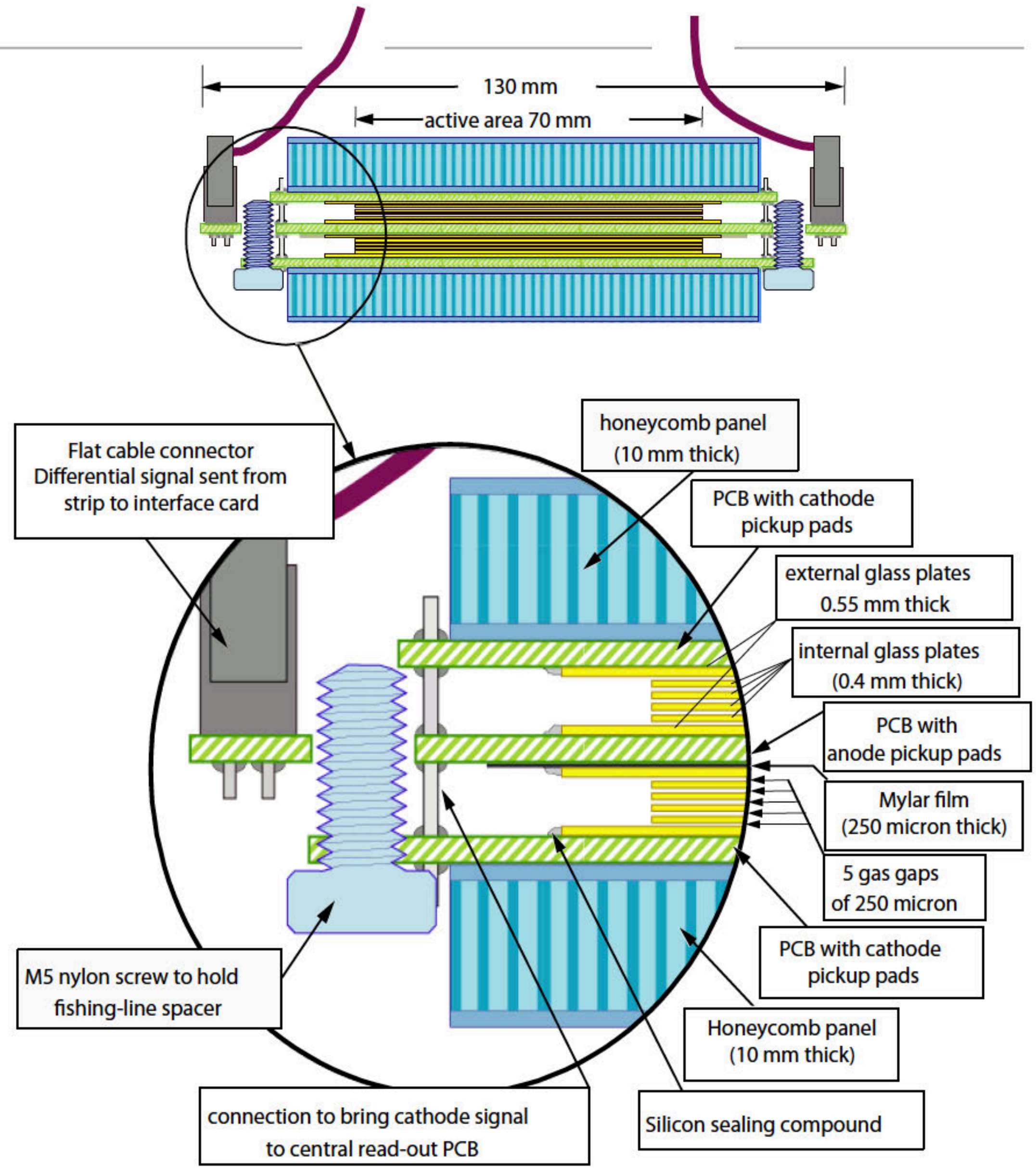

Performance of the ALICE RPC-based Time-of-Flight system

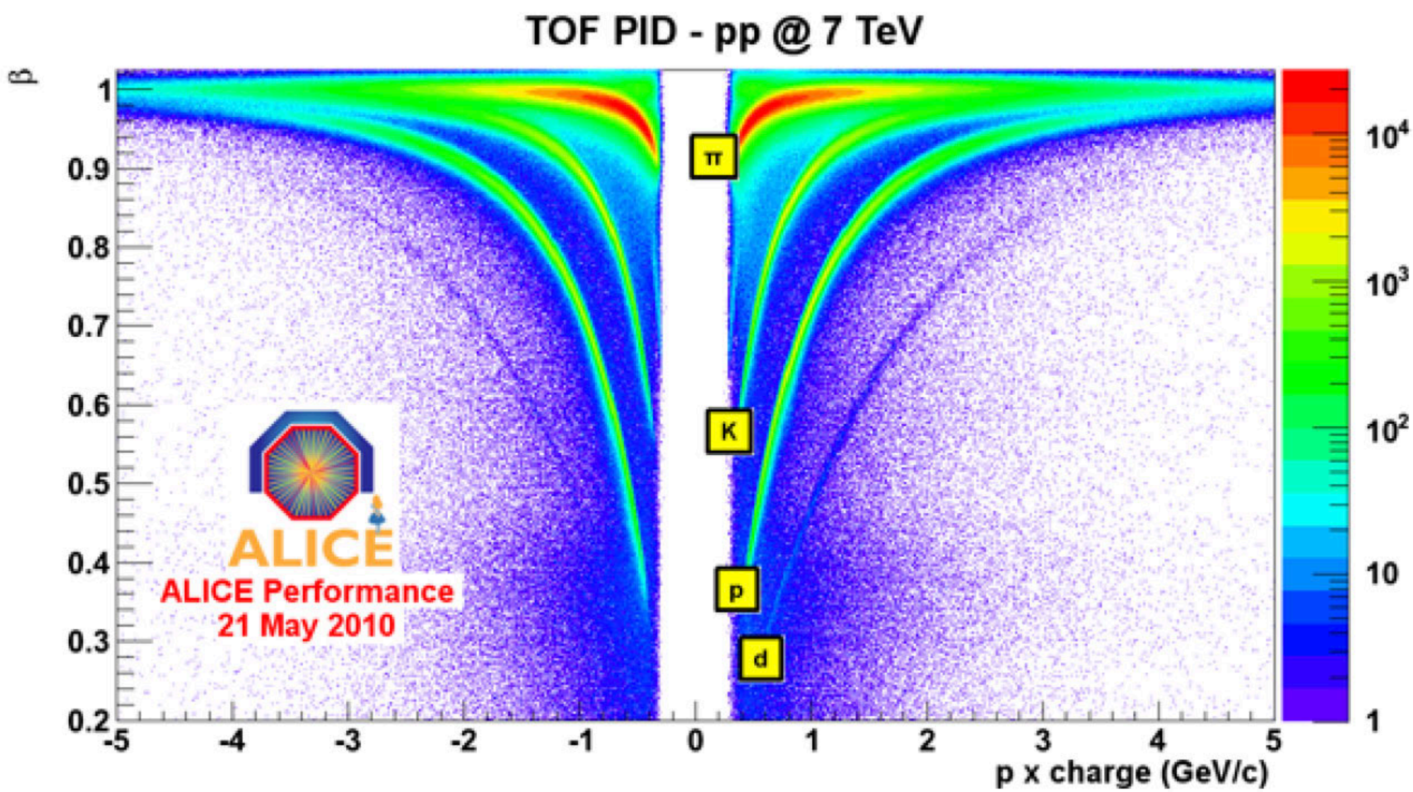

Velocity $\beta = v/c$, as measured with the ALICE TOF detector as a function of the particle momentum p multiplied with the sign of the electric charge for a data sample taken at $\sqrt{s}$ = 7 TeV pp collisions (from C. Lippmann, arXiv:1101.3276).

Why are there no data for |q| < 0.3 GeV ??

Performance of the ALICE RPC-based Time-of-Flight system

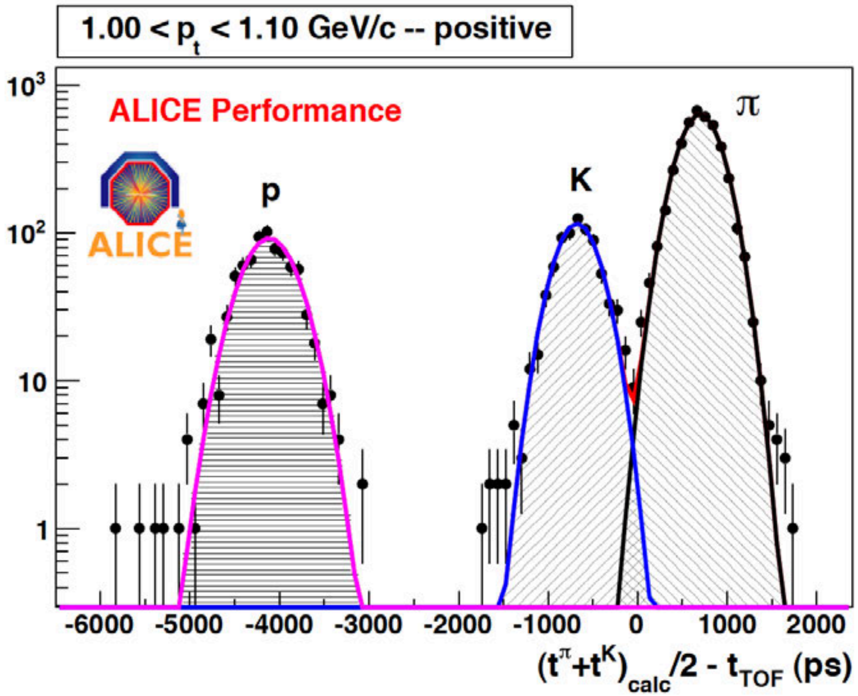

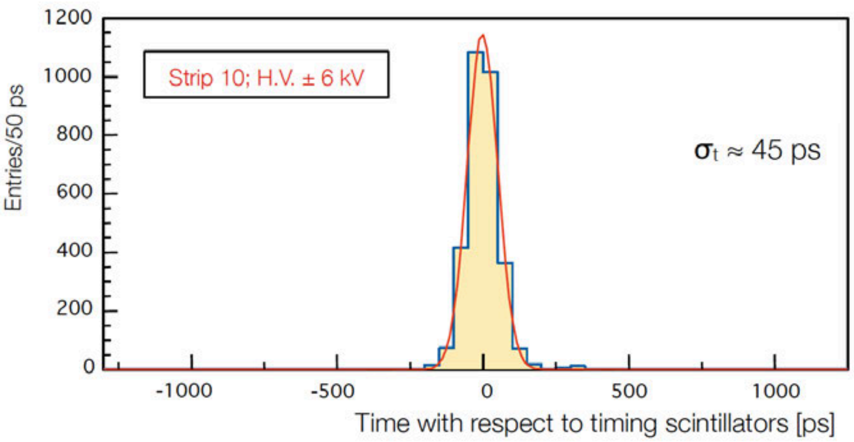

Overlap between π, K and p for a selected momentum range of $1.0 < p_T < 1.1$ GeV in the ALICE experiment (from C. Lippmann, arXiv:1101.3276).

Measured time resolution of the ALICE ToF system (from data 2010)

9.3 Particle Identification via Ionization measurement (dE/dx)

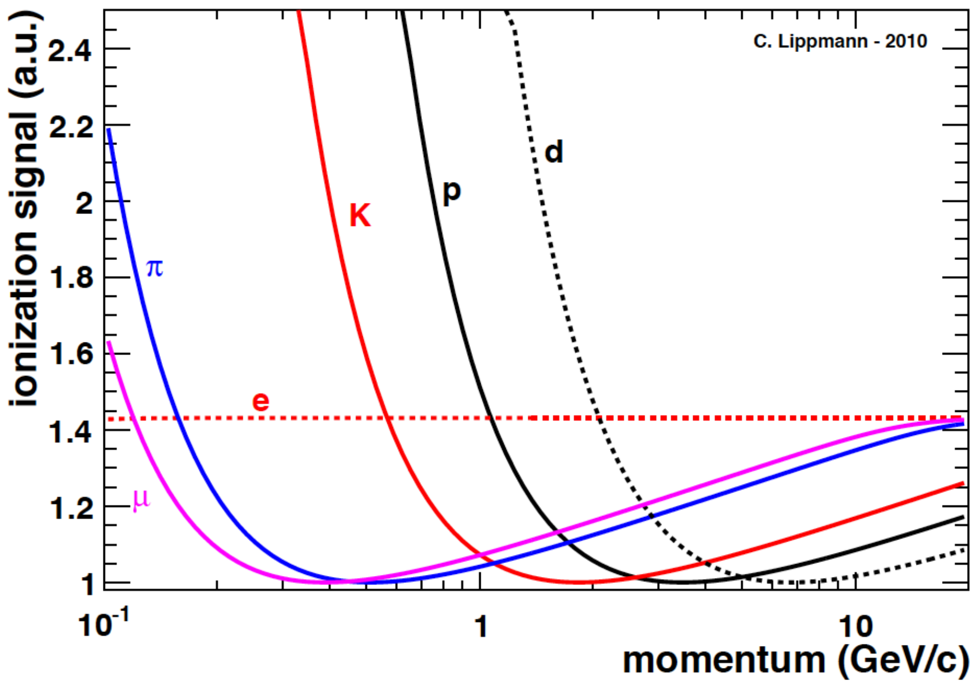

9.3 Particle Identification via Ionization measurement (dE/dx)

Basic idea: the universal (Bethe-Bloch) energy loss curve (dE/dx vs. $\beta\gamma$) splits into mass-dependent bands, if plotted as function of the particle momentum [see Chapter 2, these lectures]

$$\boxed{p = \gamma m \beta c}$$

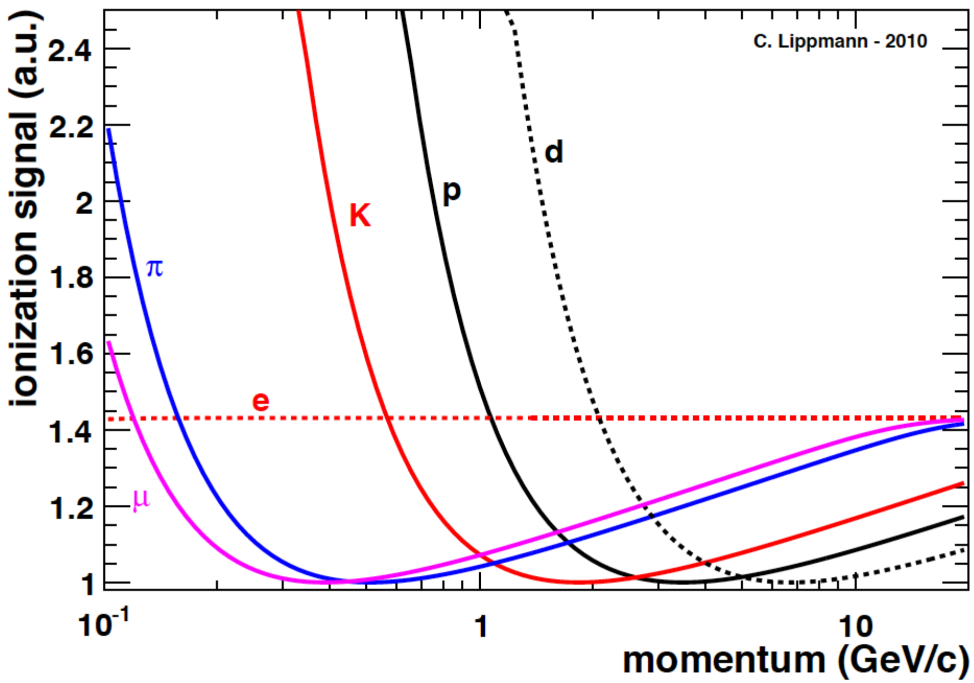

→ The combined measurement of p and ionization (<dE/dx>) provides particle identification

Overlap of curves leads to "blind spots" for certain particle-ID combinations

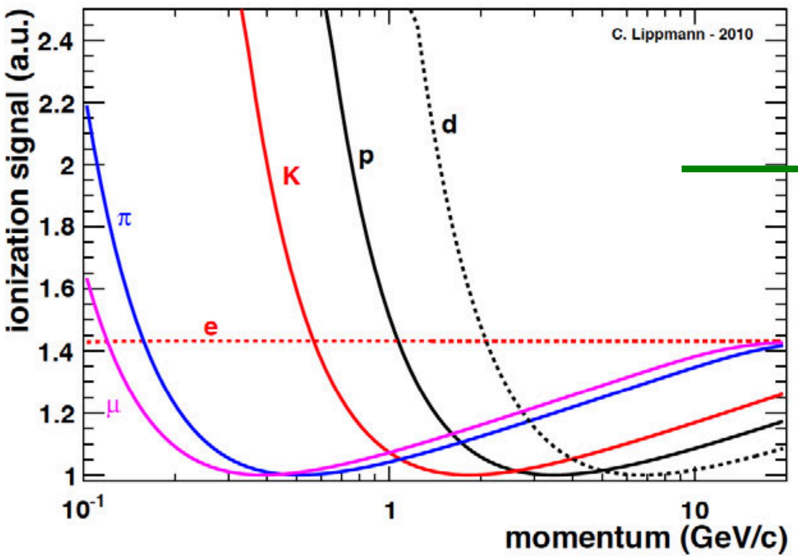

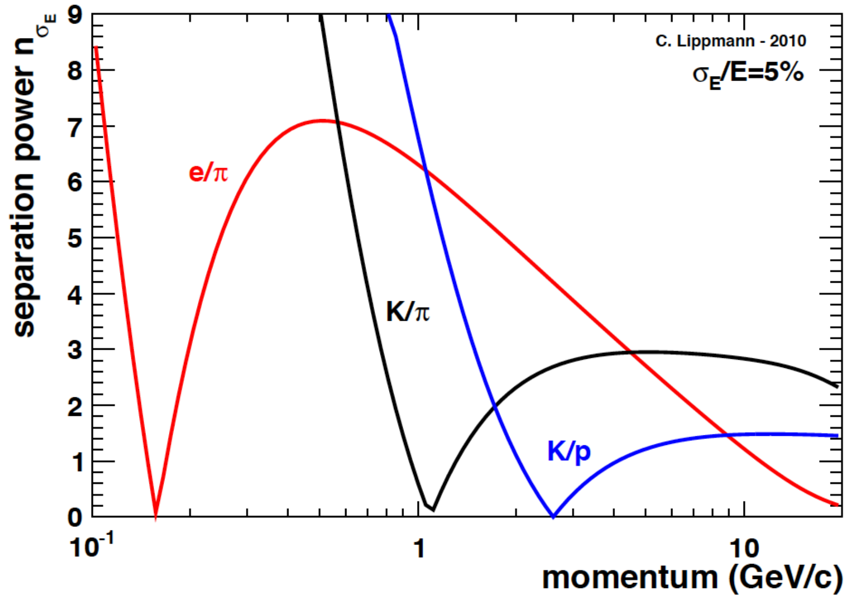

- The separation power can be defined as:
  (Depends on the achievable resolution on σ_E / <dE/dx>)

$$n_{\sigma_E} = \frac{\left\langle \frac{\mathrm{d}E}{\mathrm{d}x} \right\rangle_\mathrm{A} - \left\langle \frac{\mathrm{d}E}{\mathrm{d}x} \right\rangle_\mathrm{B}}{\left(\sigma_{E,A} + \sigma_{E,B}\right)/2}$$

- To improve the resolution, multiple measurements of the specific energy loss are performed
  → Landau / Gauss fit

  Typical values: σ_E / <dE/dx> ~3-5%

Overlap of curves leads to “blind spots” for certain particle-ID combinations

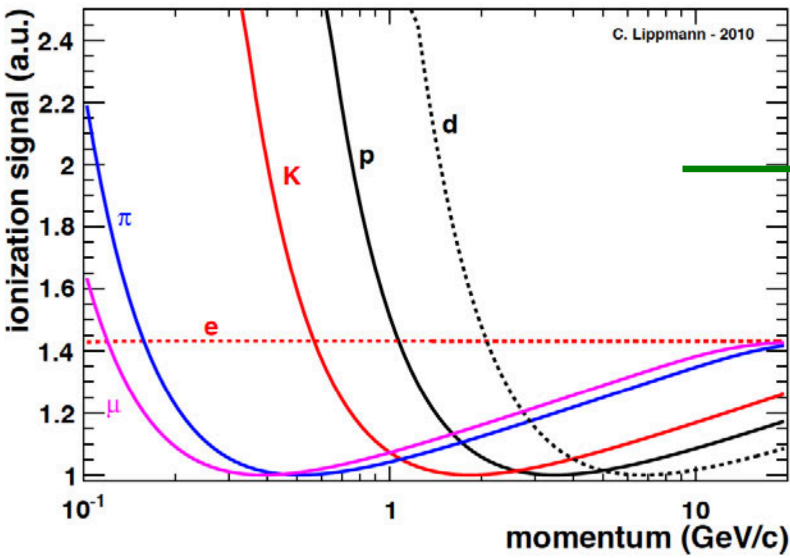

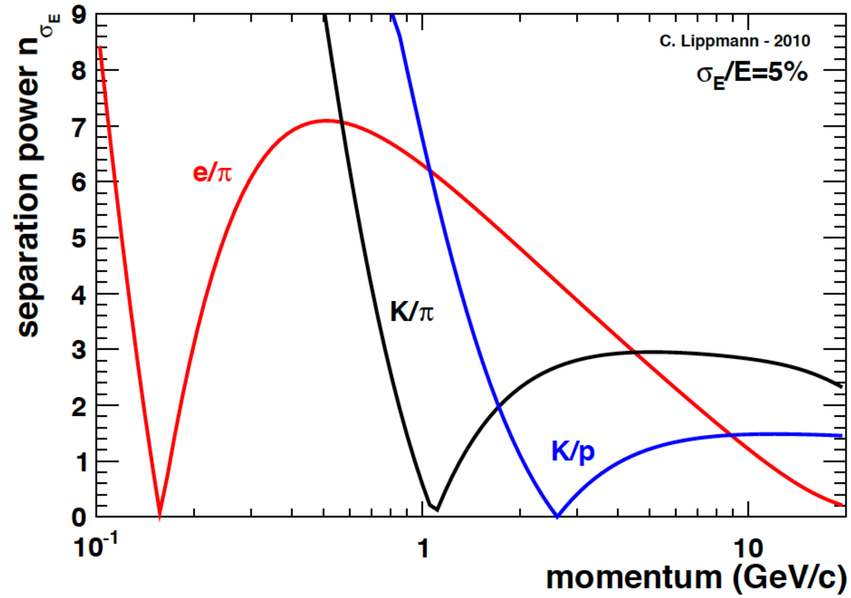

Major conclusions:

•Hadron identification works well in the low momentum region

•Problem in region of minimum ionization ($\beta\gamma \approx 3.5$)

•Moderate identification capabilities in region of relativistic rise

Example: Particle identification using dE/dx measurements

Measured quantities: particle momentum p (magnetic field)
deposited energy in a detector dE/dx

The measured values in detectors show statistical fluctuations, described by Landau / Gauss distributions, depending on the absorber thickness

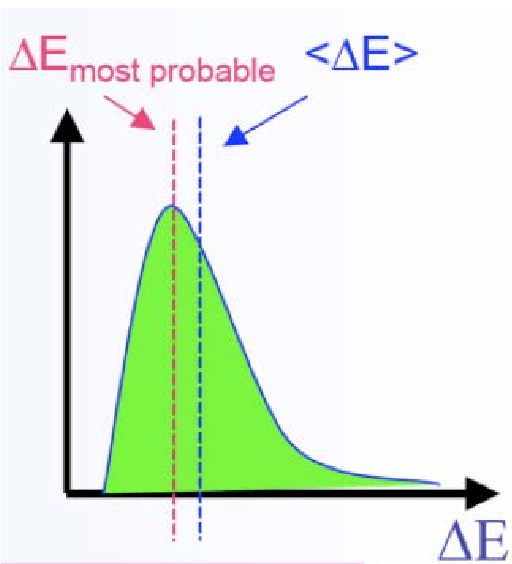

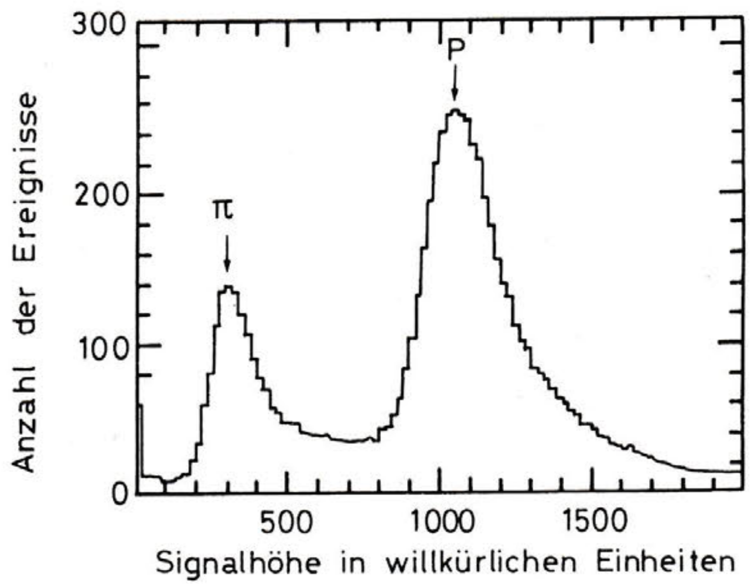

Example: distribution of the measured energy loss of a beam of pions and protons with a momentum of 600 MeV in a 3 mm thick silicon detector (from Ref. [3])

note: pions close to mip, larger signals for 600 MeV protons due to $1/\beta^2$ dependence

- Problem for particle identification: large overlap between the π and p distribution, in particular due to the asymmetric Landau distribution (large tails)
- Bethe-Bloch formula describes $<dE/dx>$; multiple repeated measurements can be used to get a better estimate of the mean dE/dx value

- Multiple, repeated, measurements of dE/dx (samplings) in consecutive detector layers → effect of Landau tail can be reduced

- Example: 100 measurements in gas detectors → mean value can be reconstructed with a relative uncertainty of $\sigma(dE/dx) / (dE/dx)$ ~2%

- Likelihood ratio methods can be used to exploit full information;

- Use Landau probability distributions and calculate likelihood for different particle hypotheses

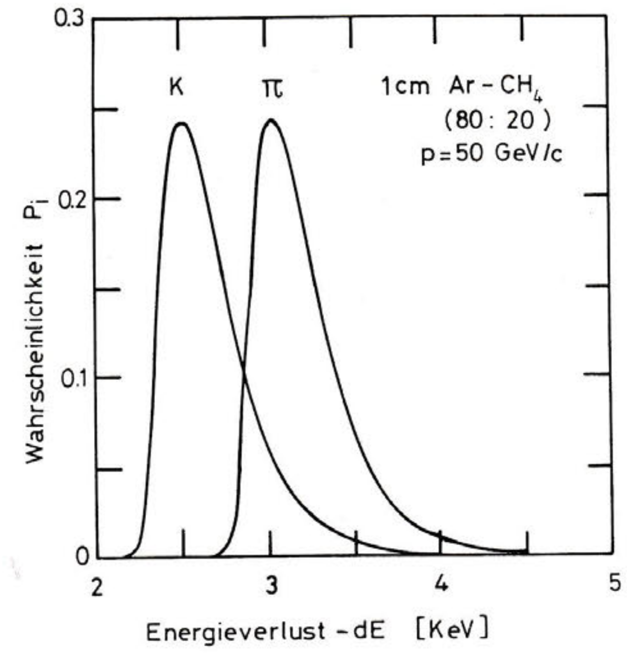

Energy loss distributions for pions and kaons with p = 50 GeV in 1 cm (argon/methane = 80/20) gas

Example: Five dE/dx measurements in an argon/methane gas detector, particle momentum 50 GeV

Calculate probabilities for the pion and kaon hypotheses

Pion hypothesis:

$$P_1 = \prod_{i=1}^{N} P_\pi^i(x_i) \,.$$

p-values in example:
(0.031, 0.236, 0.192, 0.108, 0.047)

Kaon hypothesis:

$$P_2 = \prod_{i=1}^{N} P_K^i(x_i)$$

p-values in example:
(0.124, 0.061, 0.025, 0.013, 0.006)

Probability for pion:

$$P = \frac{P_1}{P_1 + P_2}$$

for example considered here: P = 0.998

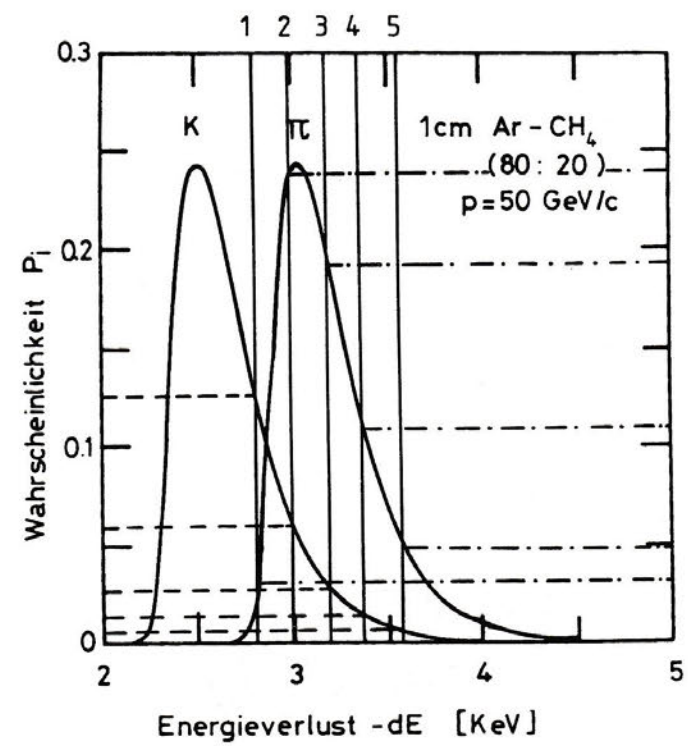

Example for π/K separation using five dE/dx measurements and Landau probability distributions;
The probabilities for the two hypotheses are indicated (from Ref. [3])

Particle Identification performance of the ALICE TPC

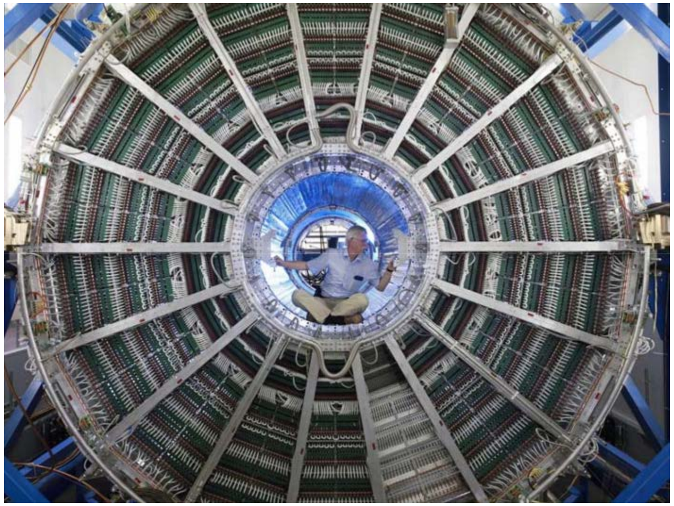

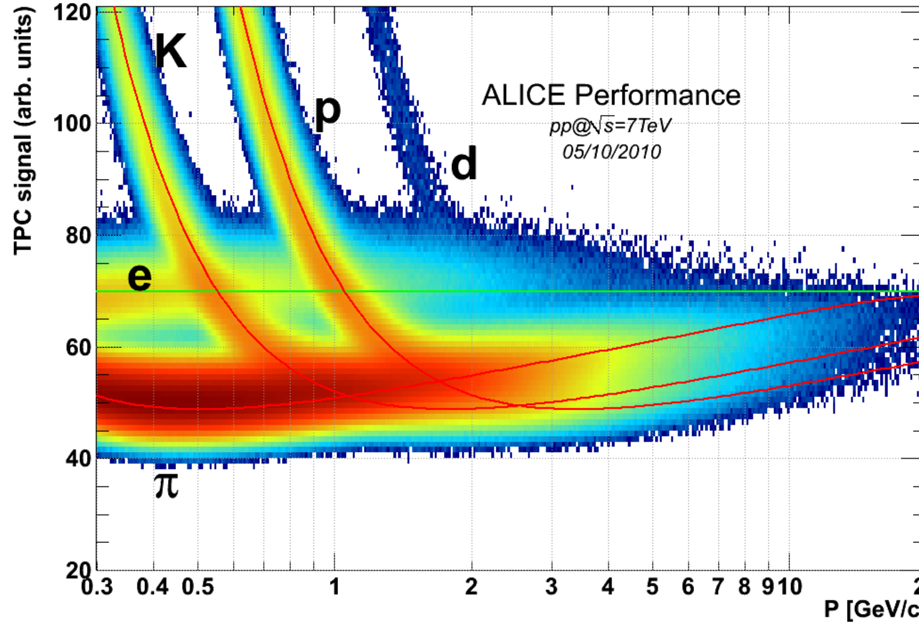

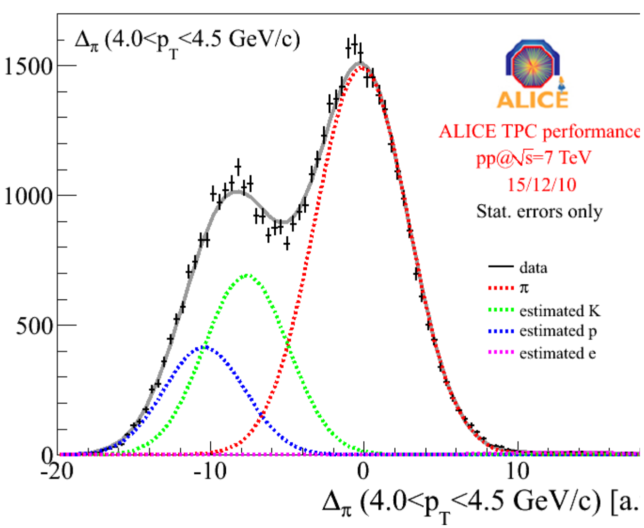

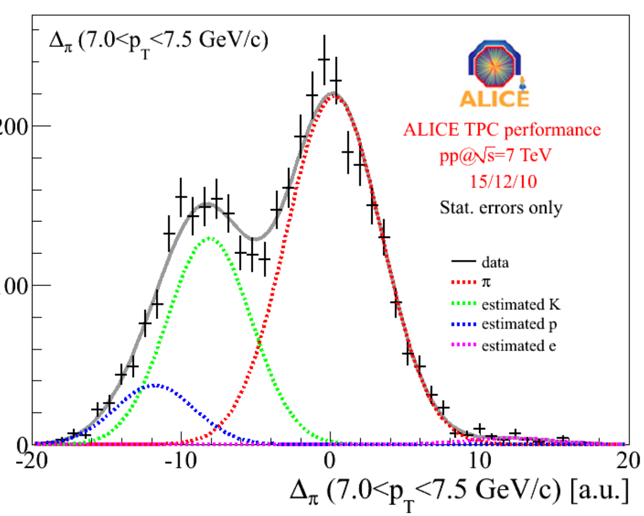

- Impressive performance for low momenta

- Separation on statistical basis even possible at high momenta (relativistic rise)

→ probability assignments possible

Particle Identification performance of the ALICE TPC

- A plot from heavy ion collision data-

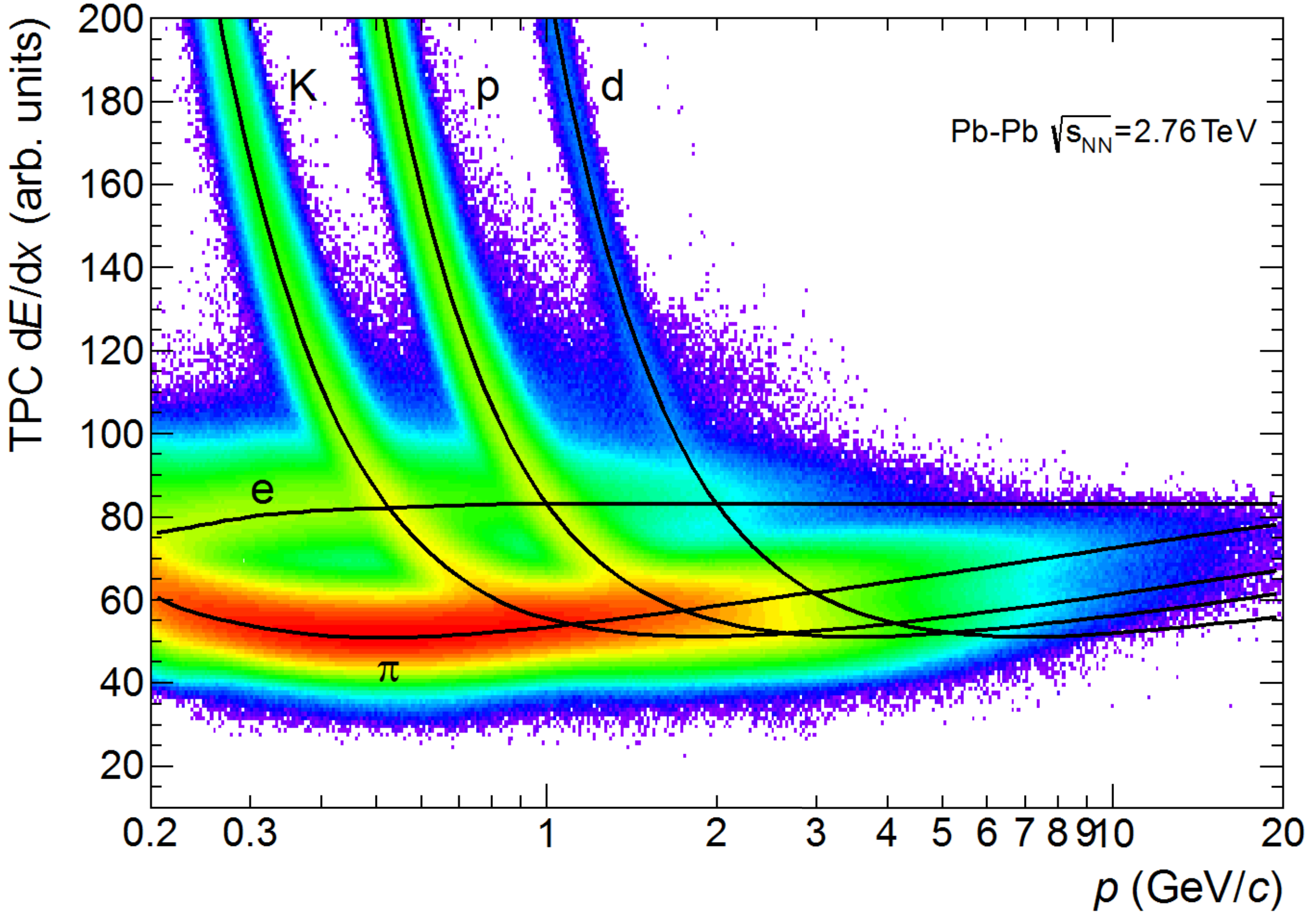

Combined ALICE Particle Identification performance

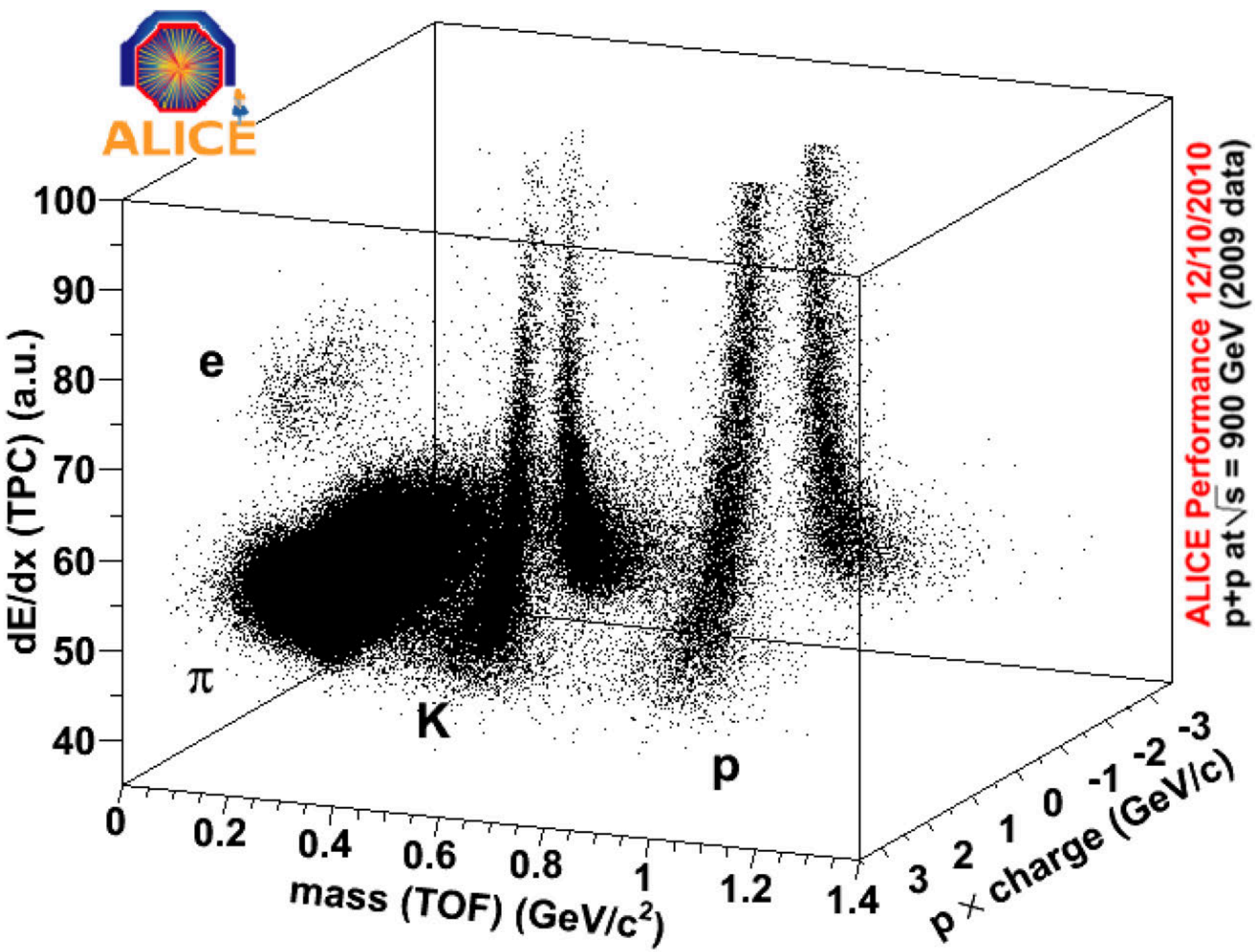

9.4 Particle Identification via Cherenkov Radiation

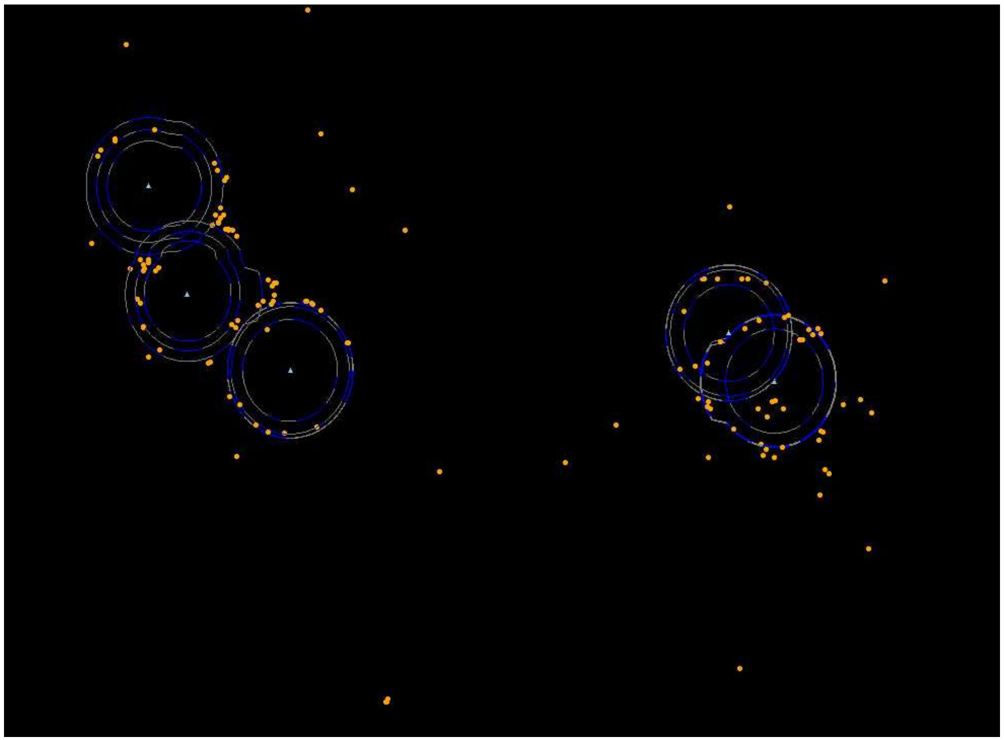

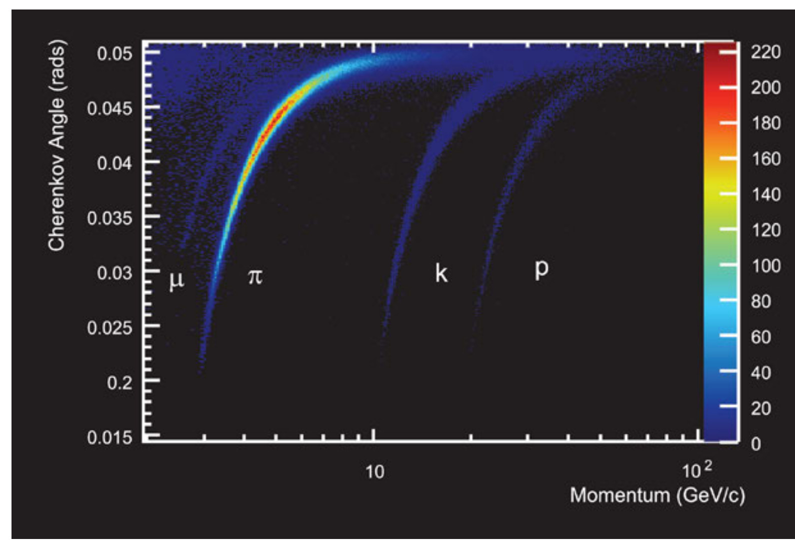

Cherenkov radiation:

Reminder:

Polarization effect ...
Cherenkov photons emitted if v > c/n ...

Cherenkov angle:

$$\cos\theta_c = \frac{1}{n\beta}$$

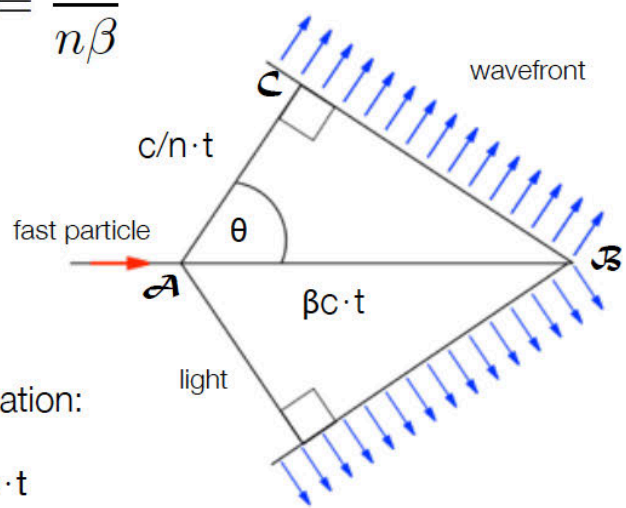

Simple
Geometric derivation:

$\mathcal{AB}$ = βc·t
$\mathcal{AC}$ = c/n·t

cos θ = $\mathcal{AC}/\mathcal{AB}$ = c/n·t/(βc·t)

= 1/nβ

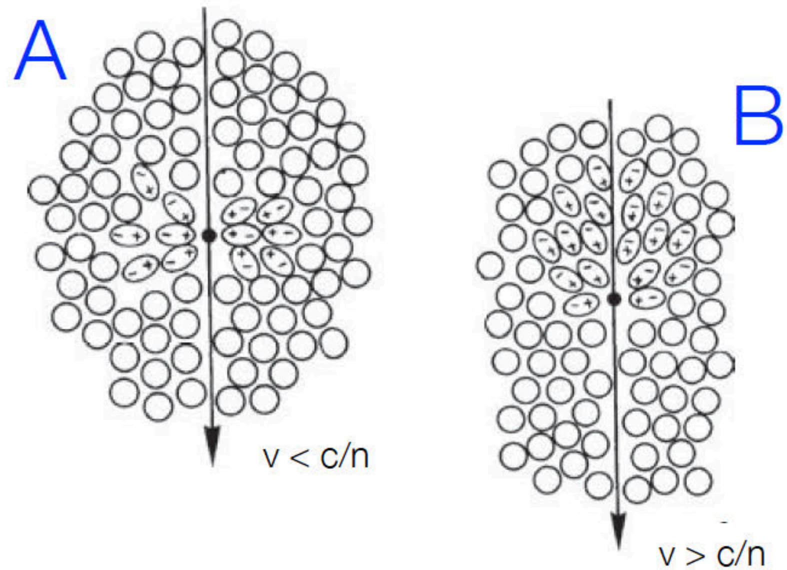

A: v < c/n

Induced dipoles symmetrically arranged around particle path; no net dipole moment; no Cherenkov radiation

B: v > c/n

Symmetry is broken as particle faster the electromagnetic waves; non-vanishing dipole moment; radiation of Cherenkov photons

Dependence of the Cherenkov angle on β:

$$\boxed{\cos\theta_c = \frac{1}{n \cdot \beta}}$$

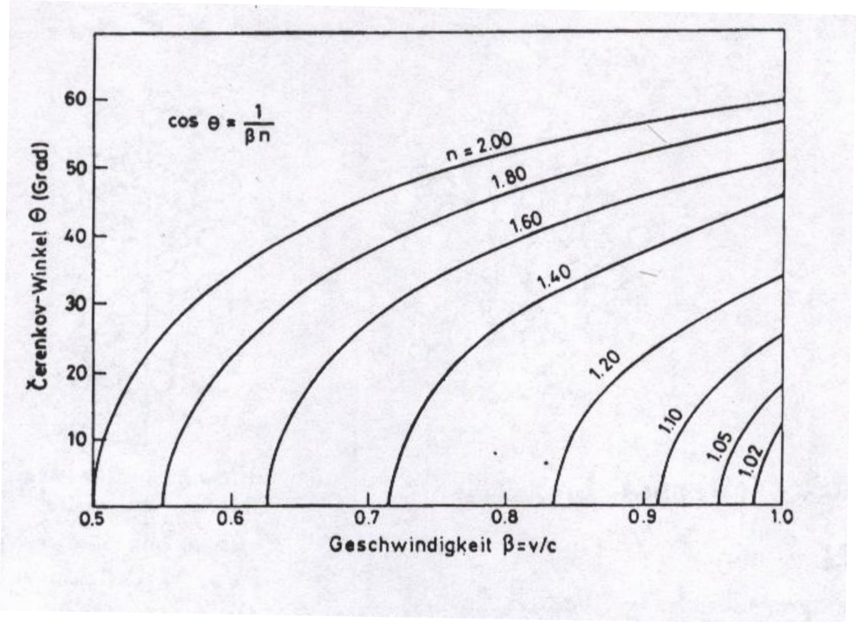

$$\theta_c^{min} = 0 \qquad \beta = 1/n$$

$$\frac{1}{n} < \beta < 1$$

$$\theta_c^{max} = \arccos\frac{1}{n} \qquad \beta = 1$$

Application for Particle Identification

(i) **Threshold counters**: measure the intensity of Cherenkov radiation and discriminate light particles that emit radiation from heavier ones that don't

(ii) **Differential Cherenkov counter**: focus only Cherenkov photons with a certain emission angle onto the detector → detect particles in a narrow β interval

(iii) **Imaging Cherenkov counters**: Measurement of the Cherenkov angle → β (particle velocity) In conjunction with add. measurements of p → particle mass

Light output:

- As already discussed in Chapter 2, the energy loss of charged particles due to Cherenkov radiation is much smaller than the ionization energy loss

$$-\left.\frac{dE}{dx}\right|_{CH} \sim 0.01 - 0.02\ \mathrm{MeV/g \cdot cm^{-2}} \quad \text{(gases)}$$

- The number of radiated photons is given by (see Jackson, Classical Electrodynamics):

$$\frac{dN}{dx} = 2\pi\alpha z^2 \int_{\lambda_1}^{\lambda_2} \left(1 - \frac{1}{n^2\beta^2}\right) \frac{d\lambda}{\lambda^2}$$

- For λ_1 = 400 nm and λ_2 = 700 nm and for z = 1, one obtains (see Grupen): (dispersion neglected, i.e. $n(\lambda)$ =const)

$$\frac{dN}{dx} = 490 \sin^2\theta_c [\mathrm{cm}^{-1}]$$

- Realistic case: An additional efficiency factor ε_{det}, which takes into account losses in the photon collection and detection efficiencies of the photon detector; Typical values: $\varepsilon_{det} \approx 0.10 - 0.40$

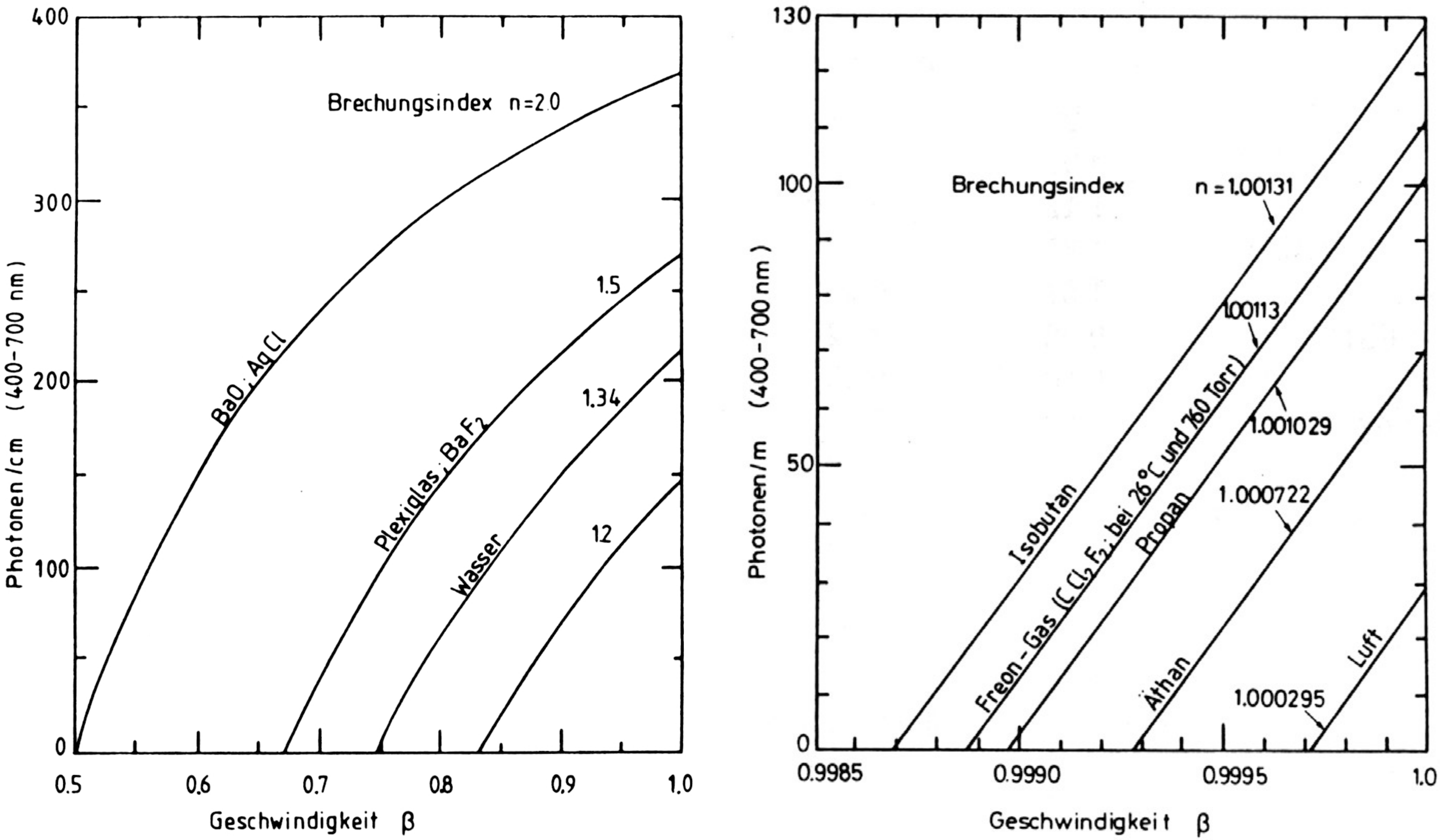

The number of photons produced by Cherenkov light emission per cm in liquids and solid state materials (left) and per m in gases (right) as a function of the particle velocity β (from Ref. [3])

Experimental requirements for Cherenkov detectors:

- **Radiator** chosen such that the Cherenkov angle varies with velocity, from threshold to the highest anticipated momentum;

  The **thickness L of the radiator** has to be chosen such that a sufficient number of photons is radiated in the particle momentum / β range of interest

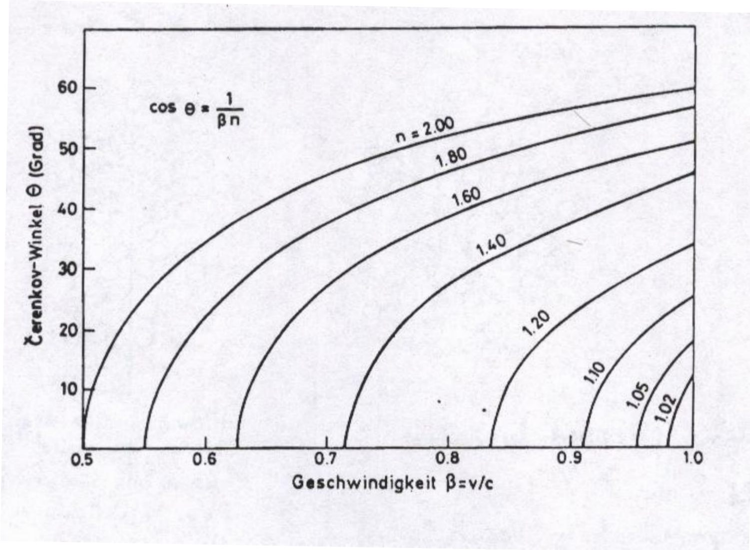

- **High quality light collecting system**
  (light guides, mirrors)
  Focusing system for (Ring) Imaging Cherenkov counters

- **High quality photon detection system**

  Typically a low number of photons is converted in photocathodes (CsI, bialkali)

(i) Threshold Cherenkov counters:

Main application: - fixed target experiments
- Separate particles based on whether they emit Cherenkov radiation of not

Threshold detection:
Observation of Cherenkov radiation ➛ $\beta > \beta_{thr}$

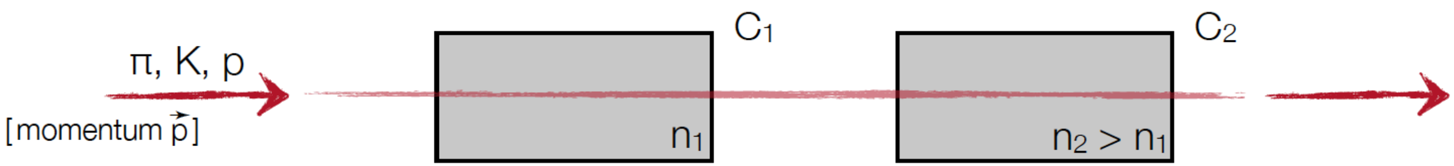

Choose n_1, n_2 in such a way that for:

n_2 : $\beta_\pi, \beta_K > 1/n_2$ and $\beta_p < 1/n_2$

n_1 : $\beta_\pi > 1/n_1$ and $\beta_K, \beta_p < 1/n_1$

Light in C_1 and C_2 ➛ identified pion

Light in C_2 and not in C_1 ➛ identified kaon

Light neither in C_1 and C_2 ➛ identified proton

(ii) Differential Cherenkov counter (an example)

Main application: - fixed target experiments
- testbeams, particle separation

Differential Cherenkov detectors:

Selection of narrow velocity interval for actual measurement ...

Threshold velocity:
[$\cos\theta = 1$]

$$\beta_{\min} = \frac{1}{n}$$

Maximum velocity:
[$\theta = \theta_{max} = \theta_t$]

Cherenkov angle limited by total reflection

$$\sin\theta_t = 1/n$$
$$\cos\theta_{\max} = \sqrt{1-\sin^2\theta_t} = 1/n\beta_{\max}$$

$$\beta_{\max} = \frac{1}{\sqrt{n^2-1}}$$

Example:

Diamond, n = 2.42 → β_{min} = 0.413, β_{max} = 0.454, i.e. velocity window of $\Delta\beta$ = 0.04 ...

Suitable optic allows $\Delta\beta/\beta \approx 10^{-7}$

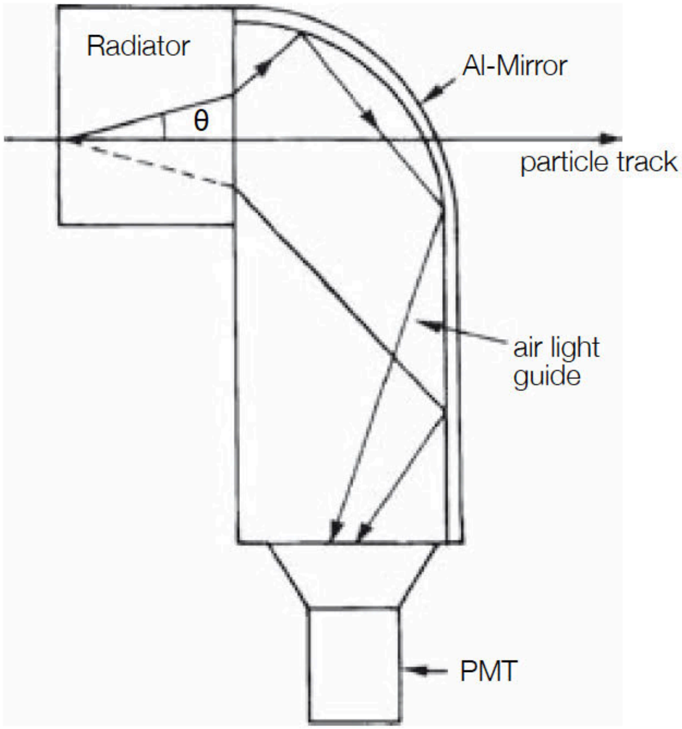

Working principle of a differential Cherenkov counter

(iii) Ring Imaging Cherenkov counter (an example)

Main application: Collider experiments (DELPHI, LHCb, ….)

Ring Imaging Cherenkov Counter

Optics such that photons emitted under certain angle form ring ...

Focal length of spherical mirror: $f = R_s/2$ ...
Cherenkov light emitted under angle: θ_C ...

Radius of Cherenkov ring: $r = f \cdot \theta_C = R_s/2 \cdot \theta_C$ ...

$$\rightarrow \beta = \frac{1}{n \cos(2r/R_s)}$$

Determination of β from r ....

Photon detection:
Photomultiplier, MWPC
Parallel plate avalanche counter ...

Gas detectors filled with photosensitive gas ...
[e.g. vapor addition or TMAE ($C_5H_{12}N_2$)]

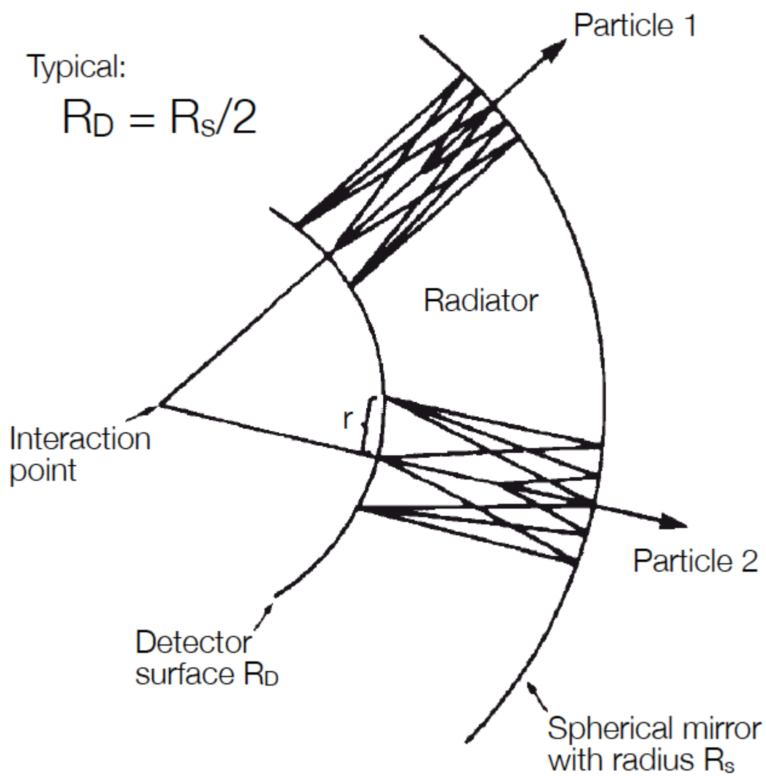

Working principle of a
Ring Imaging Cherenkov Counter (RICH)

- Ring Imaging Cherenkov Counters can be used at colliders
They allow to extend the particle ID to a much higher momentum range
→ $10 < p < 100$ GeV

- The particle mass can be reconstructed from the measured Cherenkov angle:

$$m = \frac{p}{c}\sqrt{n^2 \cos^2(\theta_C) - 1}$$

- Two-particle separation: two particles with the same momentum p and masses m_1 and m_2; measured Cherenkov angles θ_1 and θ_2

The resolution of the angle measurement determines the mass separation power

$$n_{\sigma_{\theta_C}} = \frac{\theta_{C,1} - \theta_{C,2}}{\left\langle \sigma_{\theta_C} \right\rangle}$$

For $\beta \approx 1$ the separation power can be approximated by [Particle Data Book]:

$$n_{\sigma_{\theta_C}} \approx \frac{c^2}{2p^2 \left\langle \sigma_{\theta_C} \right\rangle \sqrt{n^2 - 1}} \, | m_1^2 - m_2^2 |$$

Example: The LHCb Ring Imaging Cherenkov detector

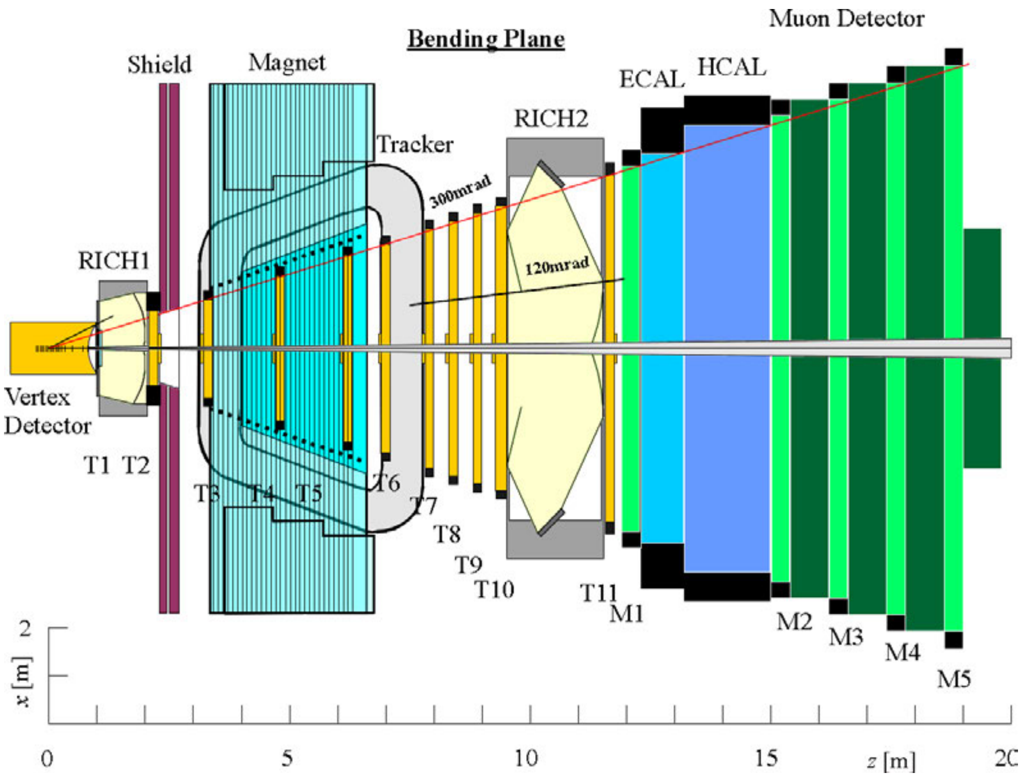

Two RICH detectors

Goal: π/K separation in the momentum range 2 < p < 100 GeV

Example: The LHCb Ring Imaging Cherenkov detector

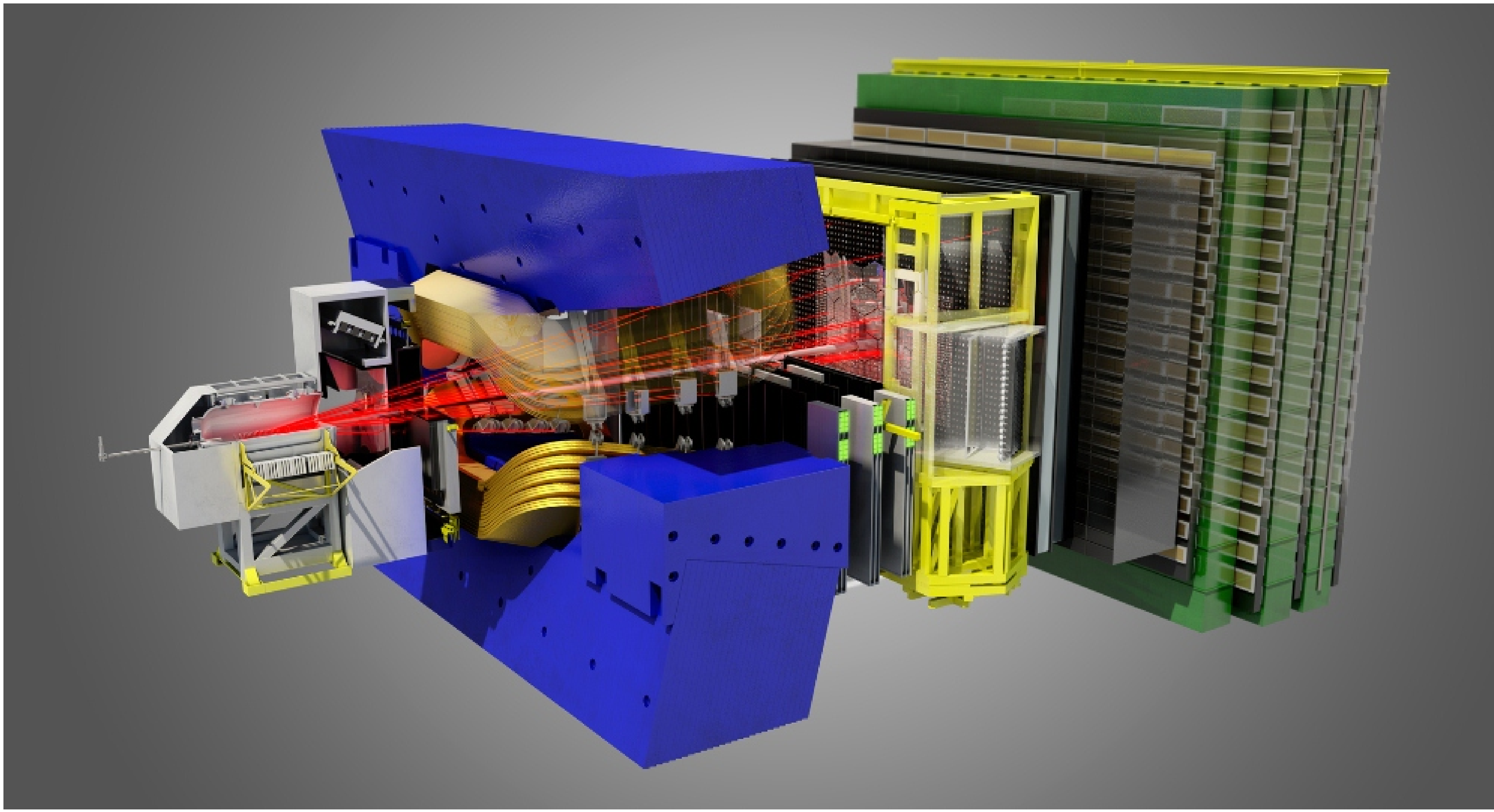

Example: The LHCb Ring Imaging Cherenkov detector

Features:

- Photon detectors are placed outside of the acceptance (250 mrad) of the LHCb detector
 (limit degradation of the momentum resolution
 of the tracking system)

- A set of spherical and flat mirrors projects the Cherenkov light onto the detector plane
 (carbon fibre material, to minimize material of mirrors
 in acceptance)

- Radiator: gas radiator C_4F_{10};
 Additional aerogel radiator in RICH-1
 → the three radiators cover the targeted momentum range

- Photon detector: (large area 4 m^2, high granularity 2.5 x 2.5 mm^2, fast readout)
 → Hybrid Photon detectors

 Quartz window with bialkali photocathode,
 20 kV acceleration + silicon pixel detector

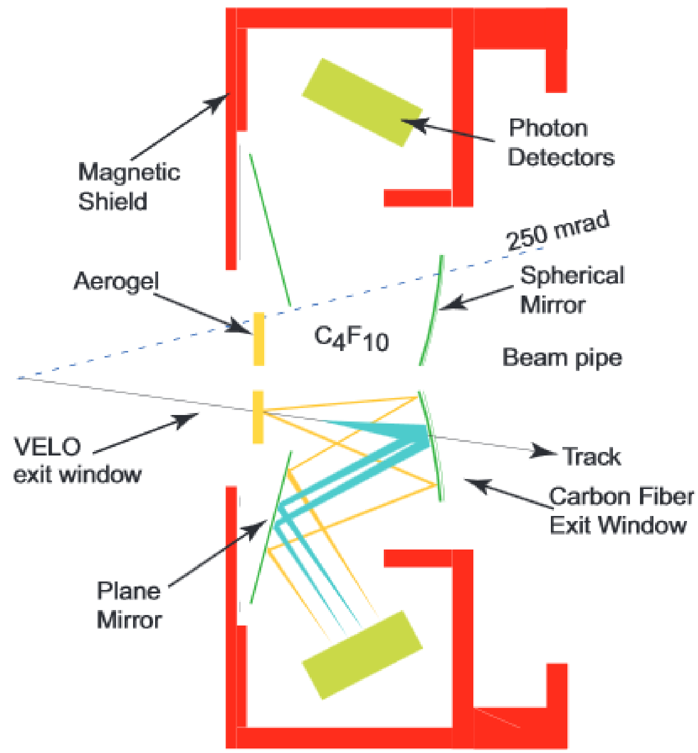

Schematic layout of the LHCb RICH-1 detector and Hybrid photon detector

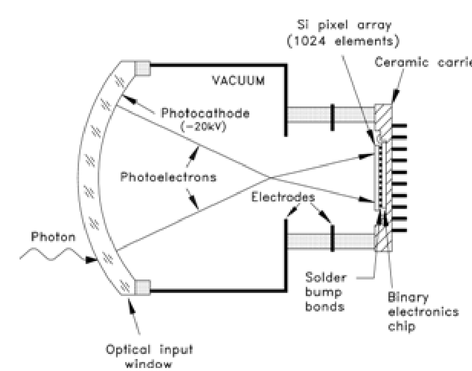

		RICH1		RICH2
		Silica aerogel	C_4F_{10}	CF_4
Momentum range [GeV/c]		≤ 10	$10 \lesssim p \lesssim 60$	$16 \lesssim p \lesssim 100$
Angular acceptance [mrad]	vertical	± 25 to ± 250		± 15 to ± 100
	horizontal	± 25 to ± 300		± 15 to ± 120
Radiator length [cm]		5	95	180
Refractive index n		1.03 (1.037)	1.0014	1.0005
Maximum Cherenkov angle [mrad]		242 (268)	53	32
Expected photon yield at $\beta \approx 1$		6.7	30.3	21.9
σ_{Θ_i} [mrad]	expected	2.6	1.57	0.67
	measured	$\sim$7.5	2.18	0.91

Some parameters of the LHCb RICH detectors

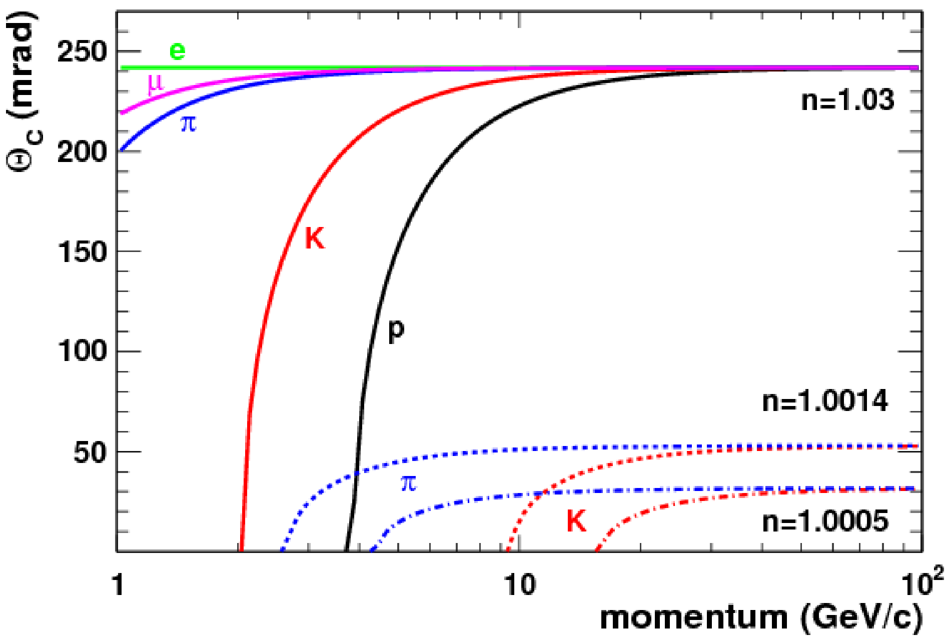

Cherenkov angles as a function of momentum for different particles for the three LHCb radiators

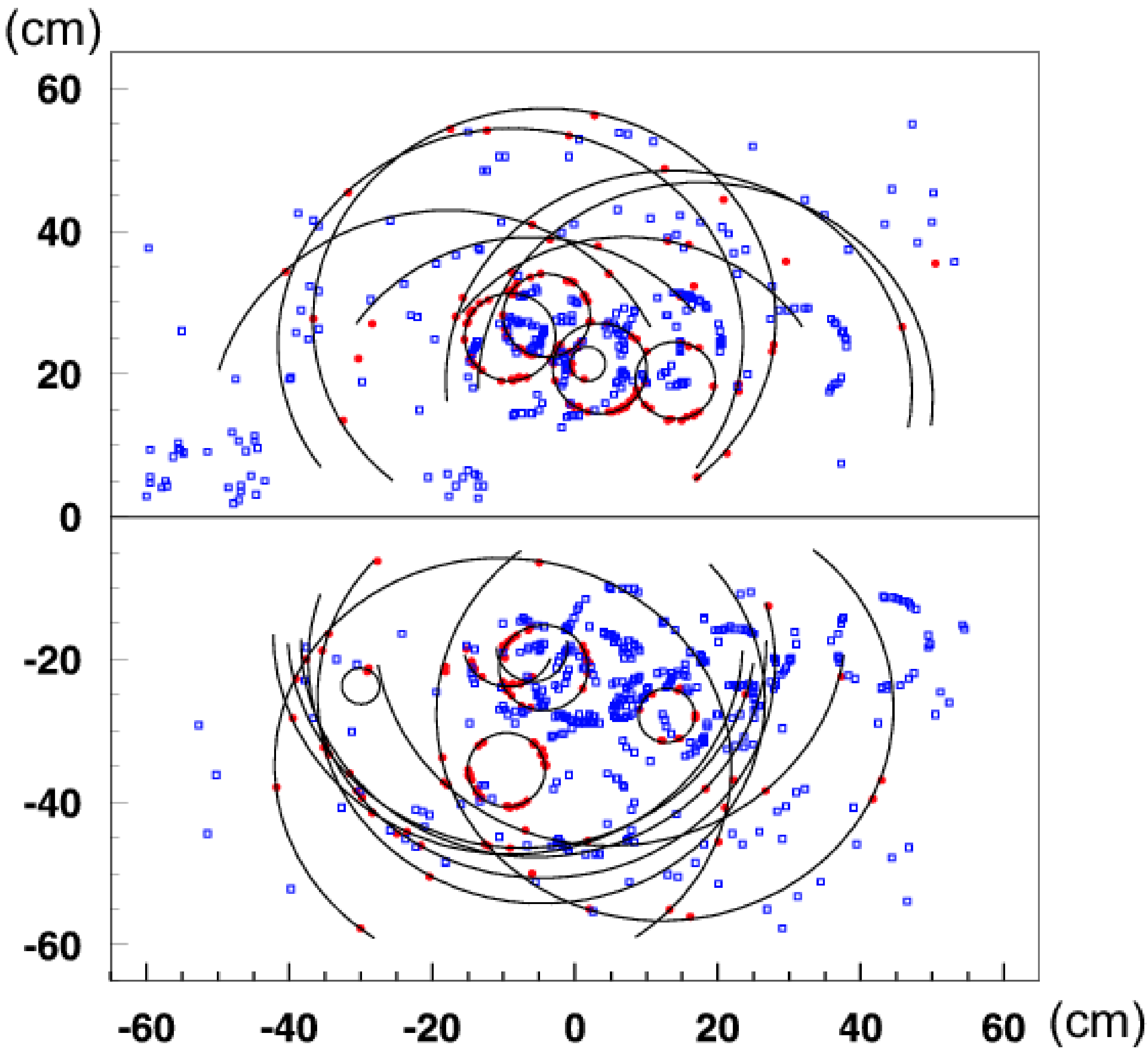

Simulated LHCb event in the RICH-1 detector
(The two photon detector planes are shown in the upper and lower halves)

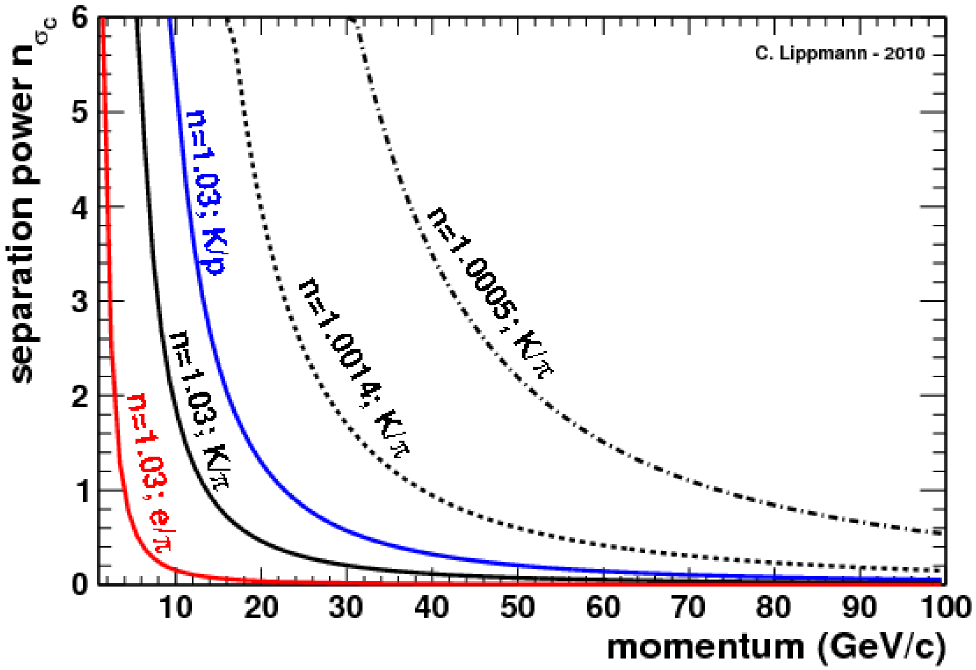

Particle separation power achievable in the LHCb RICH detectors

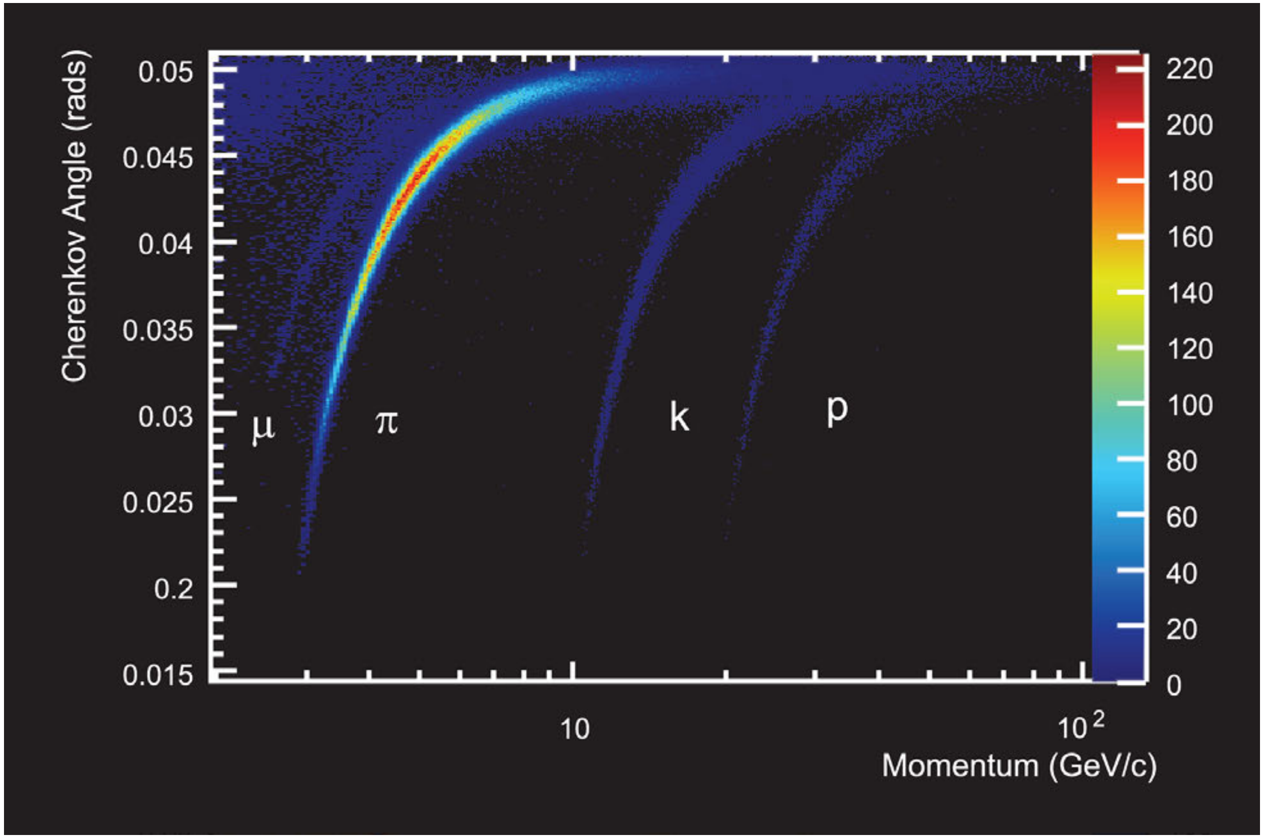

LHCb published performance plot of the RICH detectors

9.5 Particle Identification via Transition Radiation

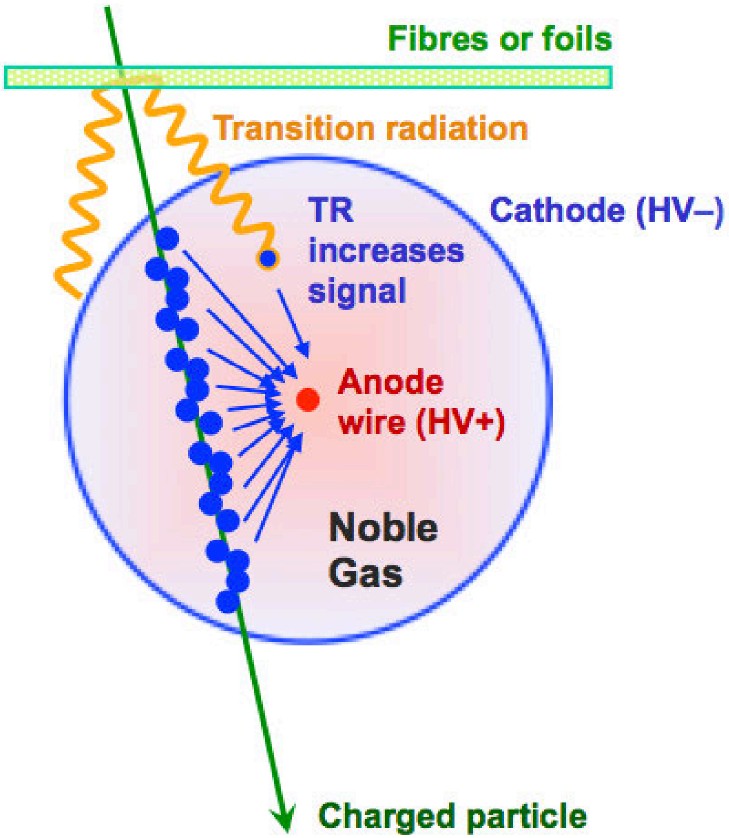

Transition Radiation:

Transition radiation occurs if a relativist particle (large γ) passes the boundary between two media with different refraction indices ...

[predicted by Ginzburg and Frank 1946; experimental confirmation 70ies]

Effect can be explained by rearrangement of electric field ...

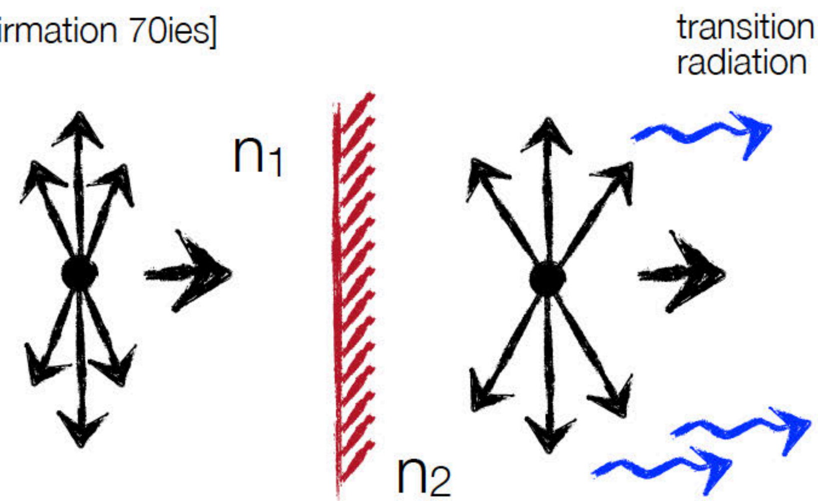

Rearrangement of electric field yields transition radiation

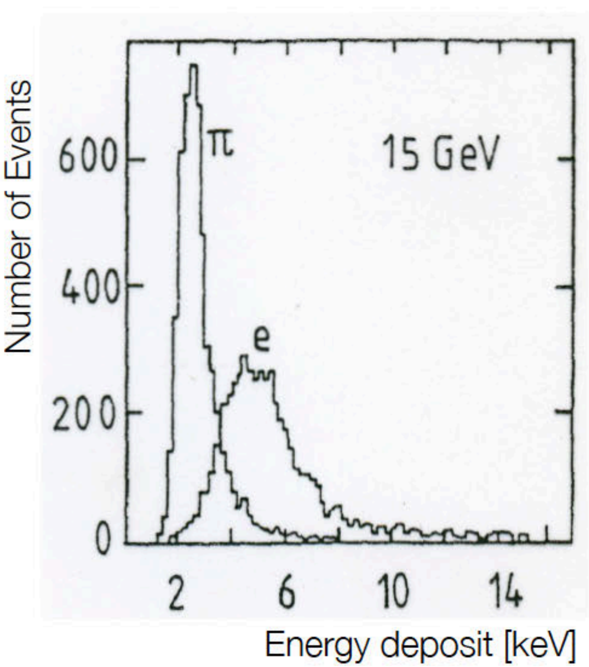

Energy loss distribution for 15 GeV pions and electrons in a TRD ...

Detection principle of Transition Radiation:

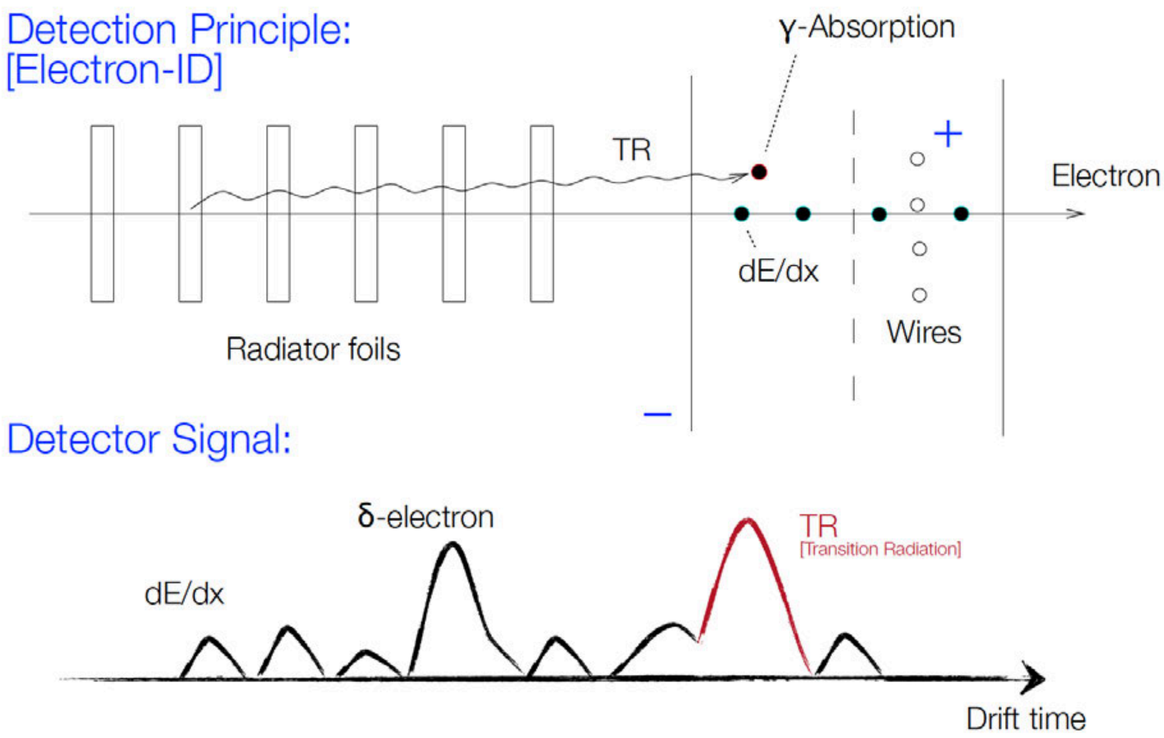

ALICE Transition Radiation detector:

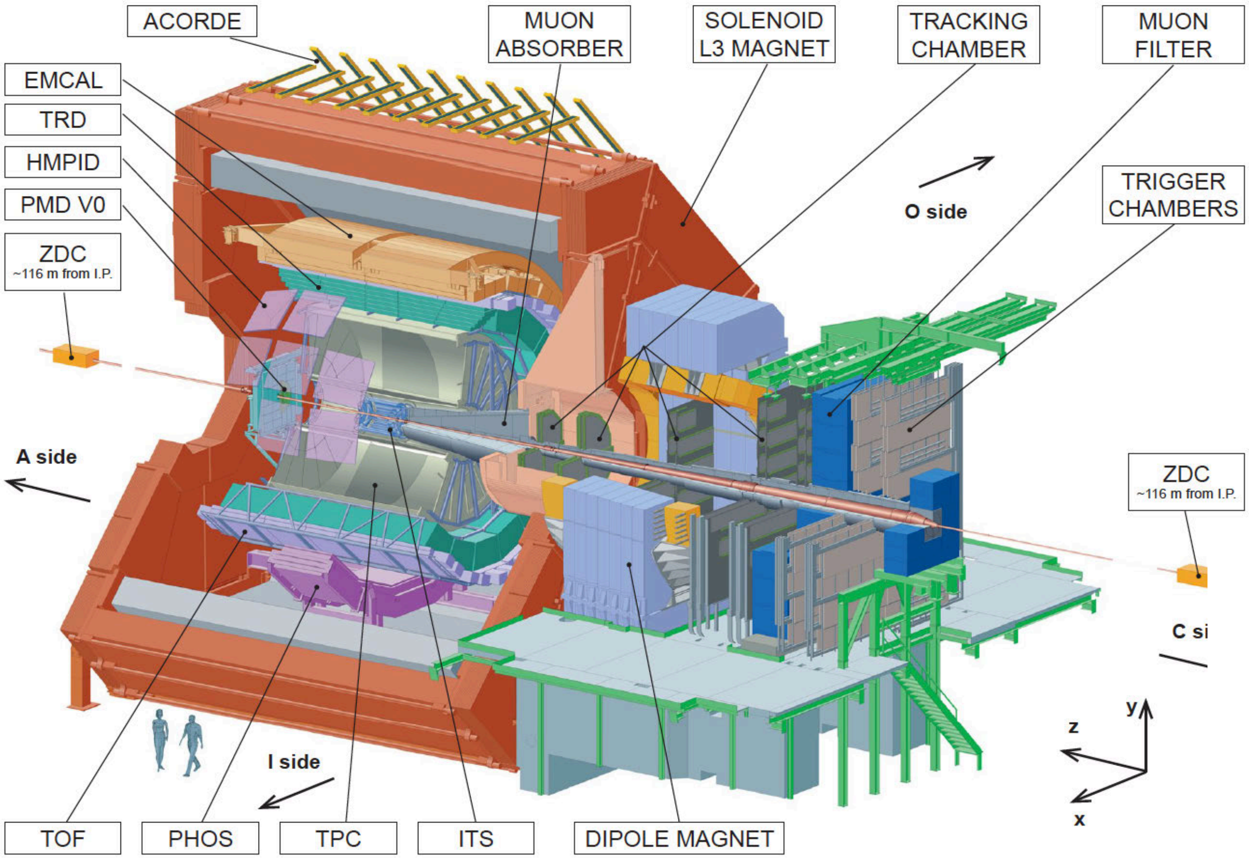

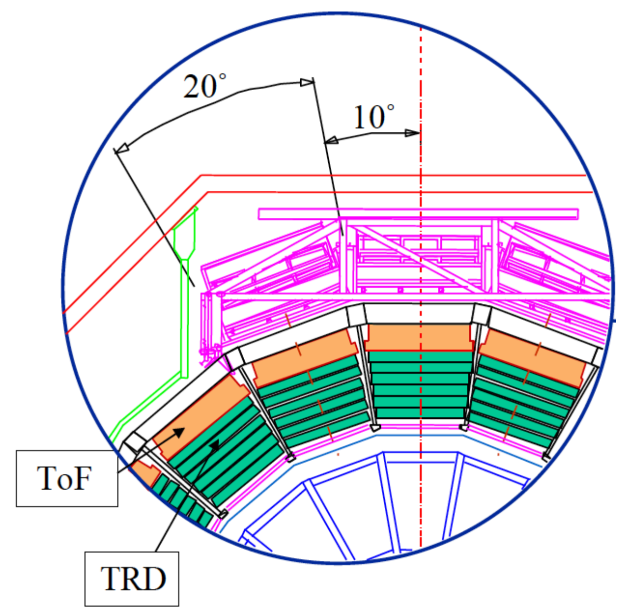

ALICE Transition Radiation detector:

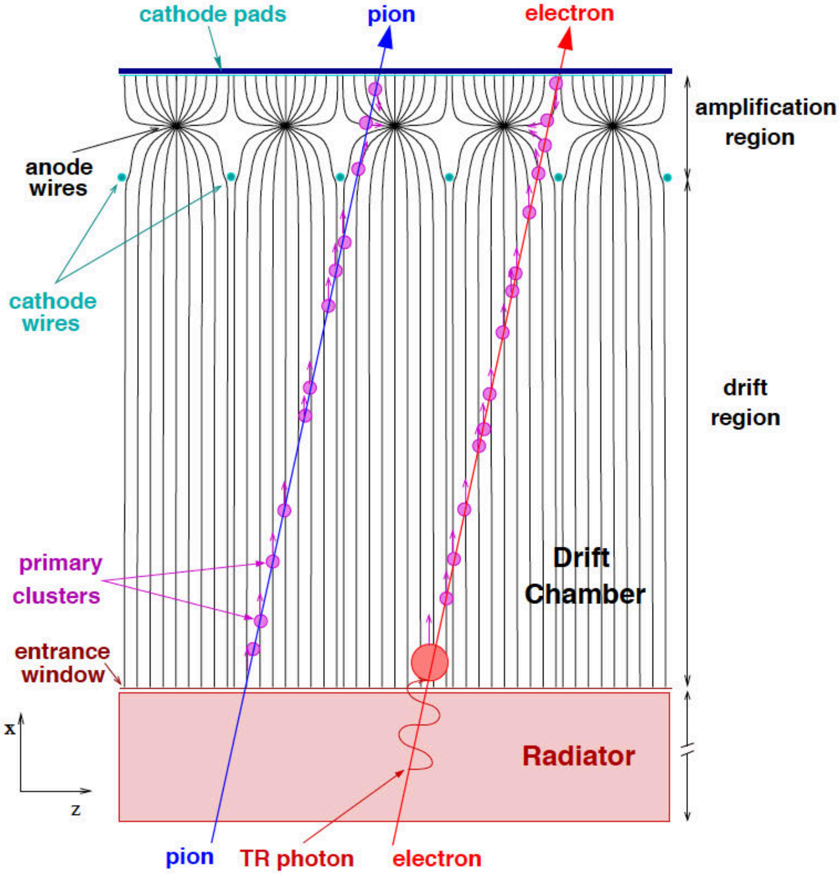

Transition Radiation [TR]
for charged Particles with $\gamma > 1000$

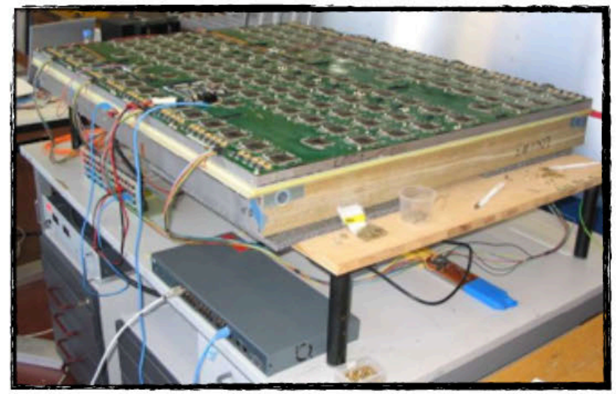

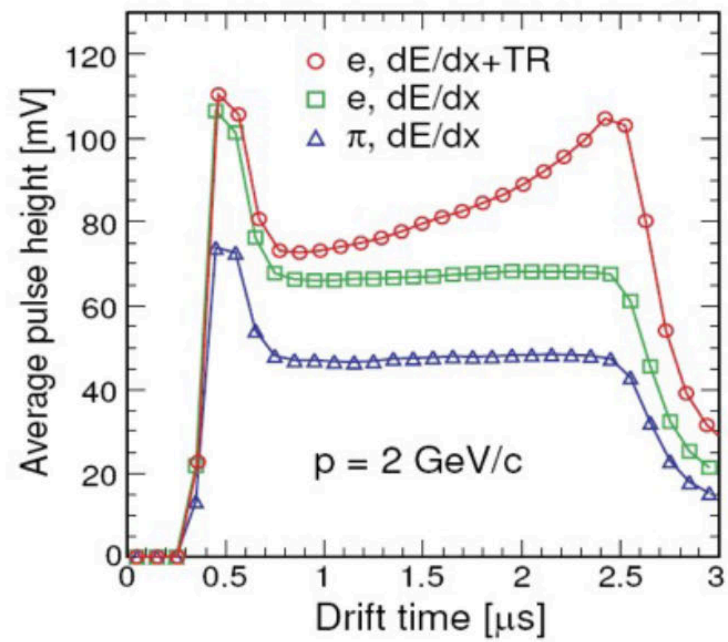

Combining Tracking with particle ID: ATLAS TRT

- e/π separation via transition radiation: polymer (PP) fibres/foils interleaved with DTs

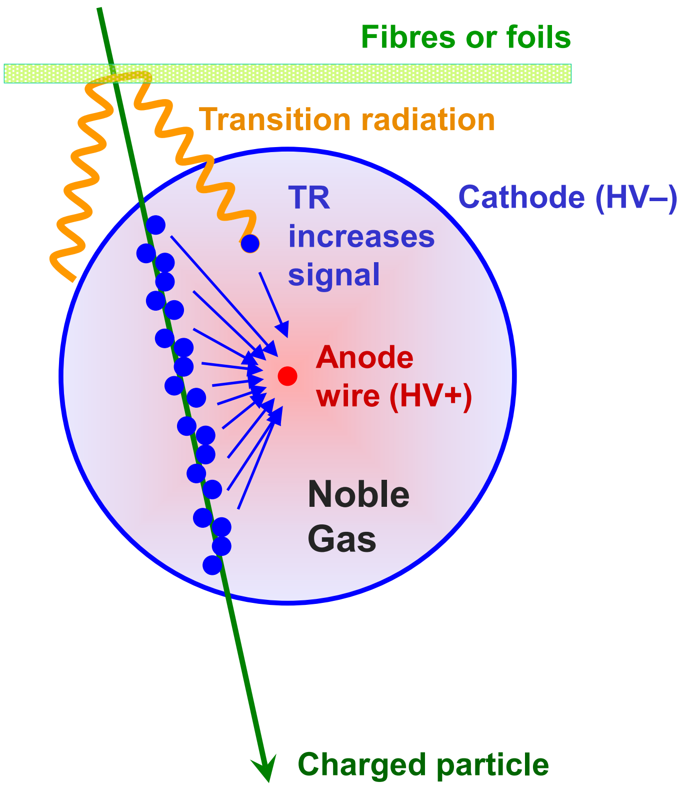

Electrons radiate → higher signal
Particle Identification by counting the number of high-threshold hits

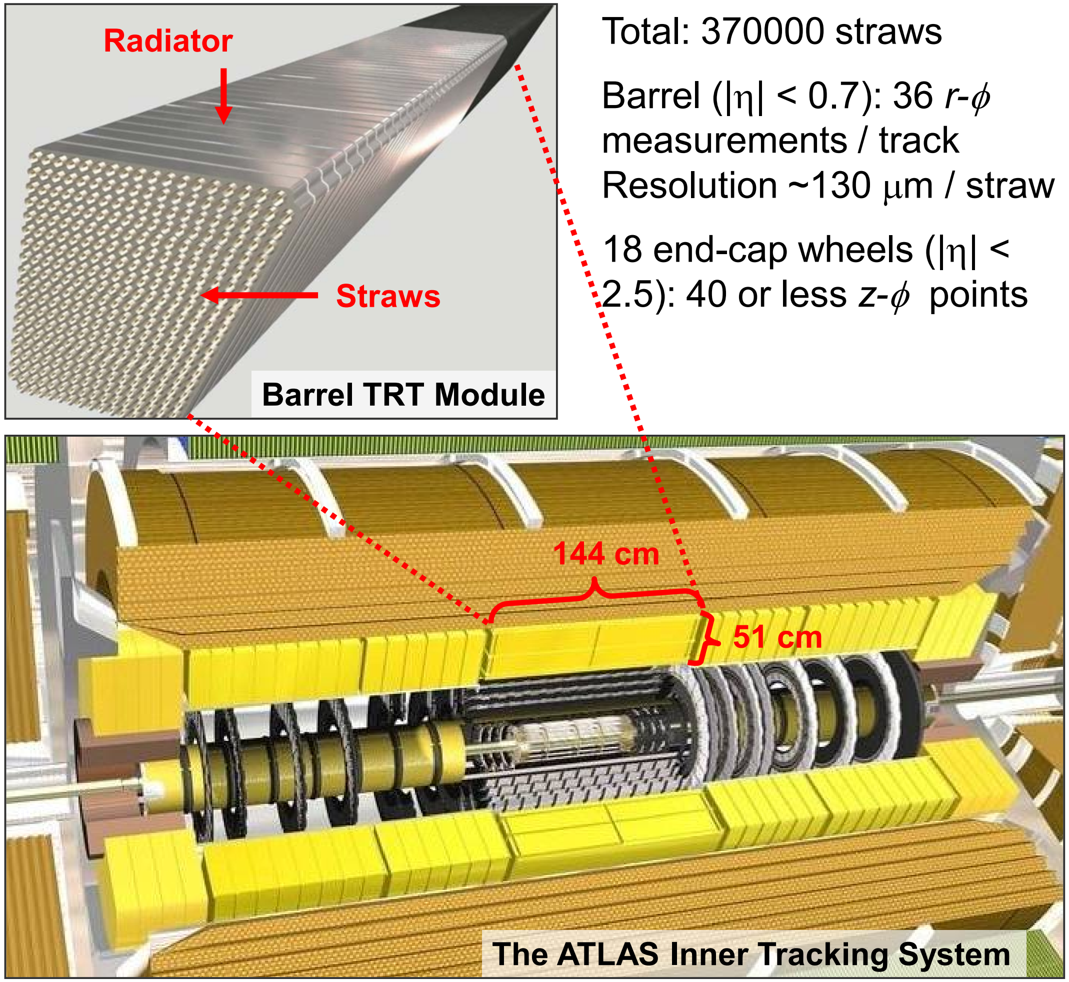

Total: 370000 straws

Barrel ($|\eta| < 0.7$): 36 r-ϕ measurements / track
Resolution ~130 μm / straw

18 end-cap wheels ($|\eta| < 2.5$): 40 or less z-ϕ points

ATLAS Transition Radiation Tracker (TRT):

- Straw tube tracker
- Inter-space filled with foam
- Different thresholds in readout:
  high threshold hits → higher probability
  for transition radiation
- Main purpose: Tracking + improved electron ID

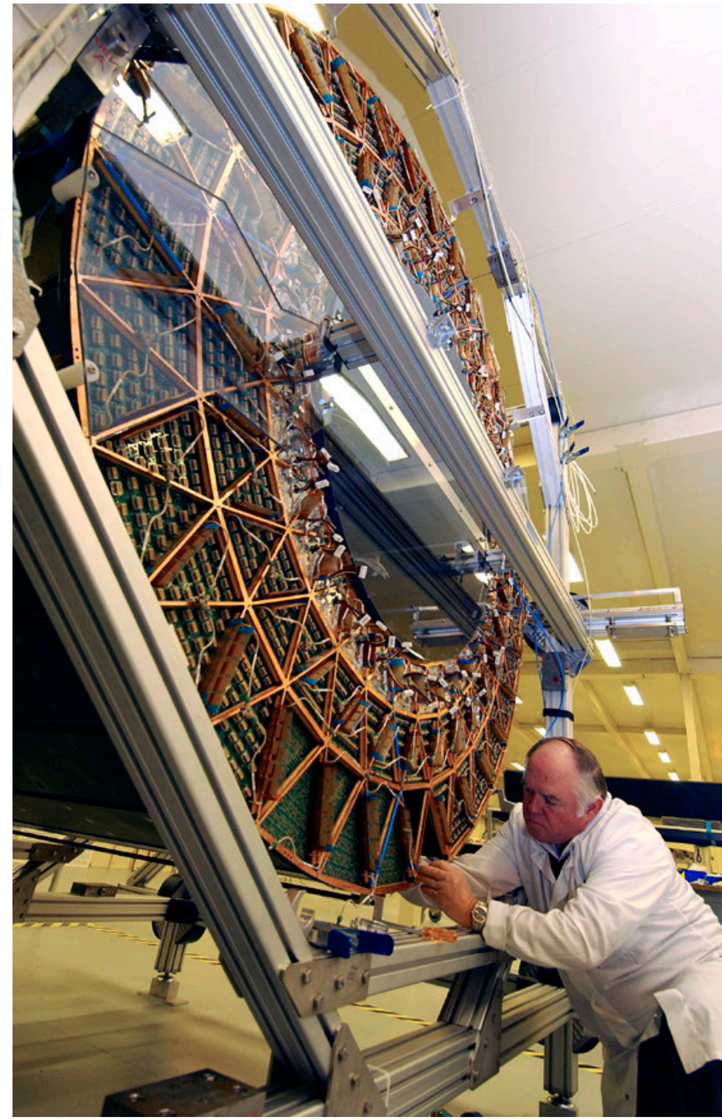

Performance of the ATLAS TRT:

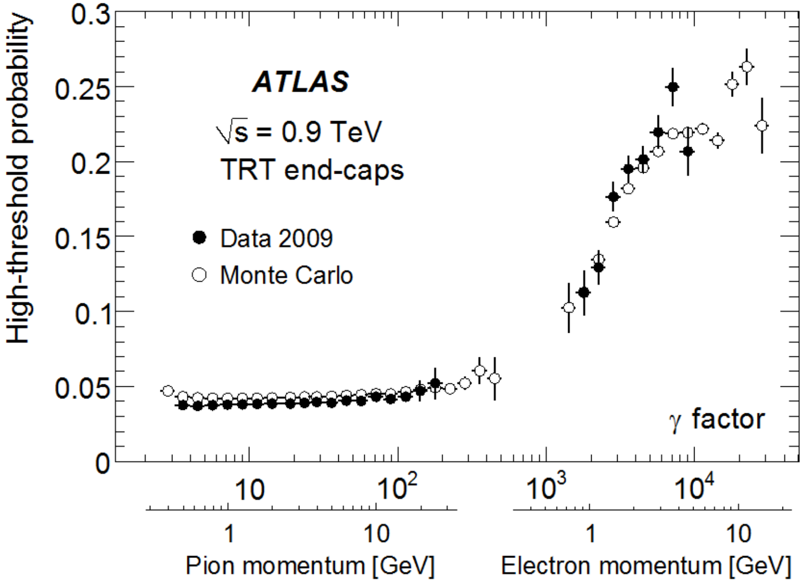

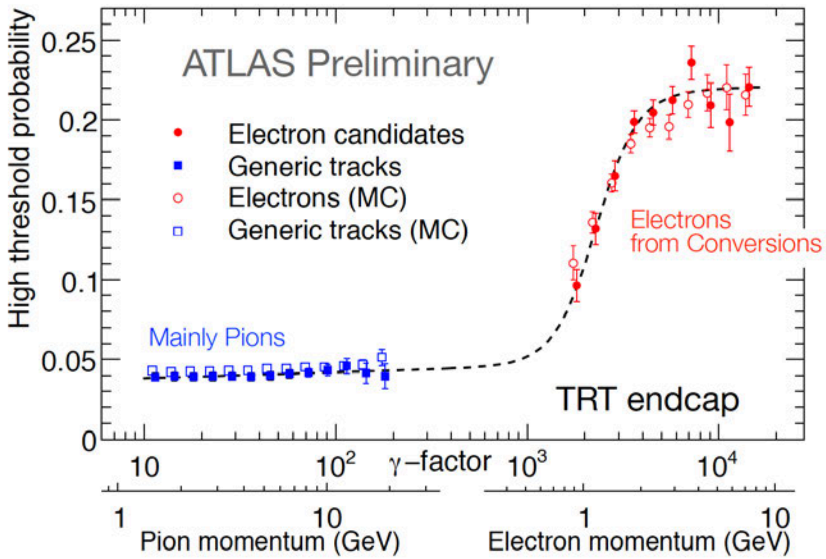

Electrons clearly visible in first LHC data (2009)
(Larger fraction of high-threshold hits)

… confirmed later by reconstructed electron candidates from conversions
(good agreement between data and Monte Carlo simulation)

Summary on Particle Identification

π/K Separation

[Comparison of different PID methods